

A SEISMIC VELOCITY MODEL OF THE CLARK HILL RESERVOIR AREA

A THESIS

Presented to

The Faculty of the Division of Graduate

Studies and Research

By

David Malcolm Dunbar

In Partial Fulfillment

of the Requirements for the Degree

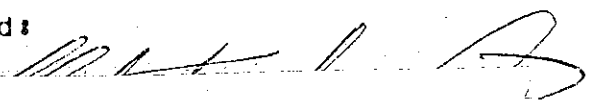
Master of Science in Geophysical Sciences

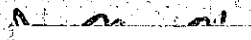
Georgia Institute of Technology

August, 1977

A SEISMIC VELOCITY MODEL OF THE CLARK HILL RESERVOIR AREA

Approved:

  
\_\_\_\_\_  
Dr. Leland Timothy Long, Chairman

  
\_\_\_\_\_  
Dr. W. Marion Wampler

\_\_\_\_\_  
Dr. Robert P. Lowell

Date approved by Chairman

8/17/1977

### ACKNOWLEDGMENTS

This thesis represents the efforts of a number of people. Dr. Leland Timothy Long served as the major director of this research. His guidance, support, and advice during the course of this work are greatly appreciated.

I wish to thank Drs. Robert P. Lowell and J. Marion Wampler for reviewing this manuscript.

I wish to thank the people who helped with the data gathering and reduction. They are (alphabetically) Mr. Stewart A. Guinn, Mr. Helmut Y. A. Hsiao, Mr. George E. Marion, and Mr. W. R. (Bill) Volz.

The U. S. Army Corps of Engineers and the Southeastern Highway Construction Company are to be thanked for their cooperation with the explosions that I used as seismic sources. The School of Geophysical Sciences supplied transportation to and from the Clark Hill area.

I also wish to thank my family for their support and patience during this undertaking. I especially want to thank the Chevron Oil Company, Geophysical Division, for allowing me to take the time necessary to complete this study.

This research was supported by the School of Geophysical Sciences and the United States Nuclear Regulatory Commission, grant number AT(49-24)-0210.

Special thanks are due the Graduate Division for waiving certain format requirements, so this thesis could be produced on the CDC Cyber 74.

## TABLE OF CONTENTS

	page
ACKNOWLEDGMENTS .....	ii
LIST OF TABLES .....	vi
LIST OF ILLUSTRATIONS .....	vii
SUMMARY .....	viii
CHAPTER 1 .....	1
Introduction	
Previous Studies	
Seismic History of the Clark Hill Reservoir Area	
CHAPTER 2 .....	8
Methods and Data	
CHAPTER 3 .....	13
Velocity Model	
Relation to Geology	
CHAPTER 4 .....	26
Comparison of Earthquake Locations	
Conclusions, Comments and Recommendations	
APPENDIX A .....	36
Table 1	
Table 2	
APPENDIX B .....	40
Travel Program	

APPENDIX C .....	45
------------------	----

Locate Program

Sample Output

APPENDIX D .....	51
------------------	----

Comparison of Earthquake Locations

BIBLIOGRAPHY .....	59
--------------------	----

## LIST OF TABLES

Table		page
1	Locations of Stations .....	36
2	Reduced Data .....	38
3	P-wave Velocity Model .....	14
4	Comparison of Old and New Models .....	52

# LIST OF ILLUSTRATIONS

Figure		page
1	Southeast Regional Map .....	2
2	Geology Map of the Clark Hill Reservoir Area ...	3
3	Map of the Clark Hill Reservoir Area .....	7
4	Map Showing Blast Site and Station Locations ...	9
5	Plot of Reduced First Arrivals .....	12
6	P-wave Velocity Model .....	15
7	Theoretical Reduced Travel Time Curve .....	17
8	Reduced First Arrivals, Georgia Side .....	19
9	Reduced First Arrivals, South Carolina Side ....	20
10	Comparison of Velocity Models .....	22
11	Plot of Travel Time Curves for Increasing Depths	27
12	Plot of Relocated Epicenters .....	28
13	Plot of Epicenters as Determined by Denman's Model .....	30
14	Projection A°-A .....	31
15	Projection B°-B .....	33



## SUMMARY

A local seismic velocity model was developed for the Clark Hill Reservoir Area using refraction data. This area has been the site of a large number of earthquakes.

The shallow P-wave velocity is a continuous function consisting of three zones. The velocity in each zone was modeled as a continuous linear increase in velocity with depth. The first zone extends from the surface (elevation 0.13 km) to 0.17 km, the second from 0.17 to 0.57 km and the third from 0.57 to 5.0 km. Depths are measured from sea level. The velocity at the surface is 4.55 km/sec, at 0.17 km it is 5.80 km/sec, at 0.57 km it is 6.10 km/sec and at 5.0 km it is 6.42 km/sec. Raypaths for the model penetrate to a depth of 3.37 km for the most distant arrivals. When this model is combined with the regional velocity model, the near-surface model represents a high-velocity seismic channel. Further evidence for such a channel is provided by the complex nature of seismic arrivals in the Clark Hill area.

The Georgia Tech earthquake location program, Doall, has been modified to use this velocity model. An unexpected result of this model is that the travel time curve for a near-surface focus crosses the curves for other depths. This leads to stability problems in the location of shallow

earthquakes.

Eighty-one earthquakes were relocated. A planar structure was found with a strike of N 50 E and a dip of 57 NW. Approximately fifty per cent of the relocated events are found within 200 meters of this structure.

## CHAPTER 1

### Introduction

The Clark Hill Reservoir Area (CHRA) is in the Piedmont Crystalline Province and is located on the Georgia-South Carolina border approximately 55 km northwest of Augusta, Georgia. Figure 1 is a regional map showing the location of the CHRA. The rocks of the CHRA are of metamorphic and igneous origin and of Precambrian to Paleozoic age. The most prominent rock types in the northwestern half of the area are granites and gneisses. In the southeastern half, the rocks are mostly volcanic in origin (see Figure 2). Denman (1974) gives a good description of the rock units and additional references.

The purpose of this study has been to measure seismic travel times in the CHRA and to develop a velocity model to fit the travel time data. A secondary objective was to detect differences in seismic velocities among the different rock units present in the field area. The velocity model is to be used to locate the position of earthquake foci in the CHRA.

### Previous Studies

Previous work concerning regional velocity measurements has been done by Dorman (1972) and Guinn (1976).

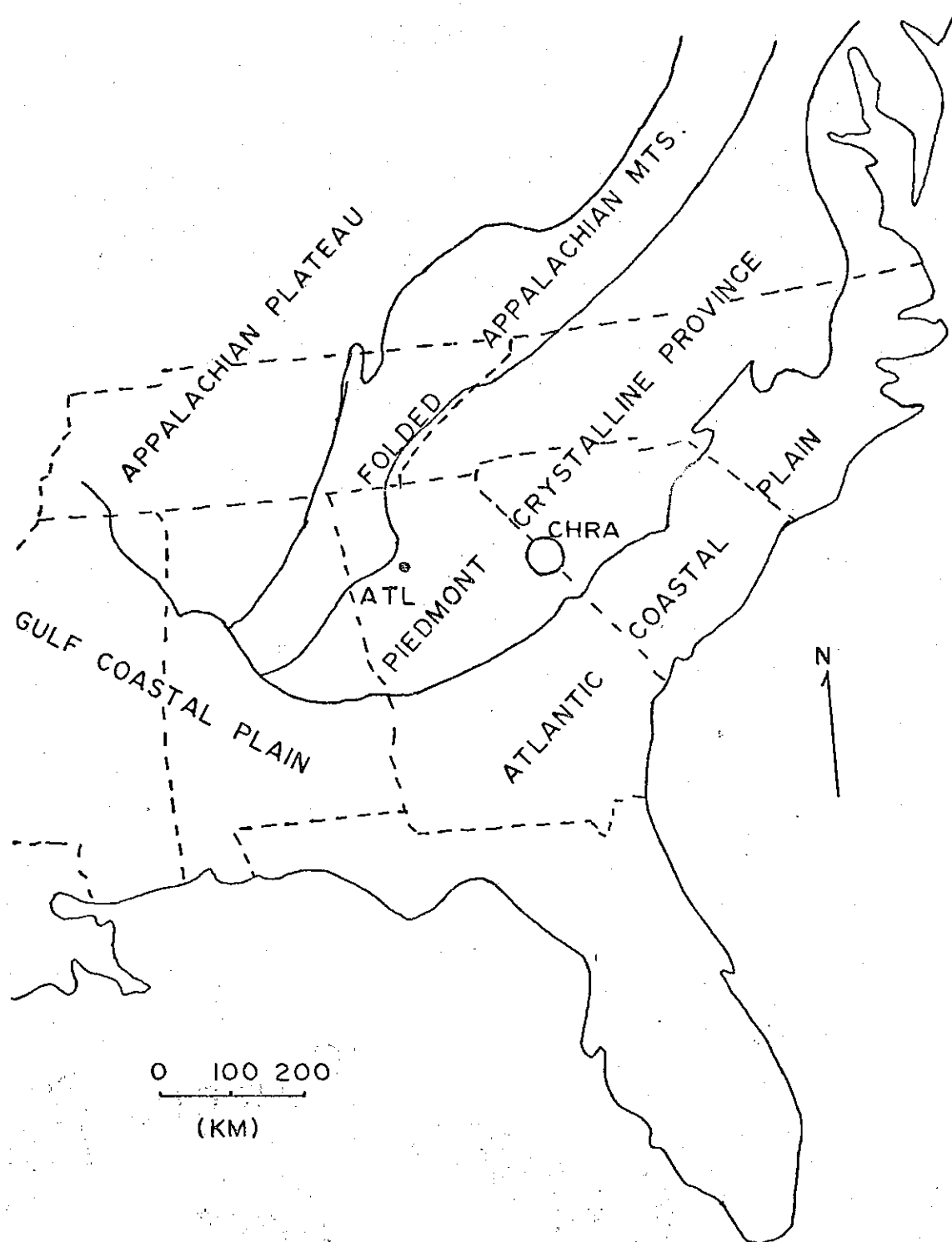


Figure 1. Southeast Regional Map

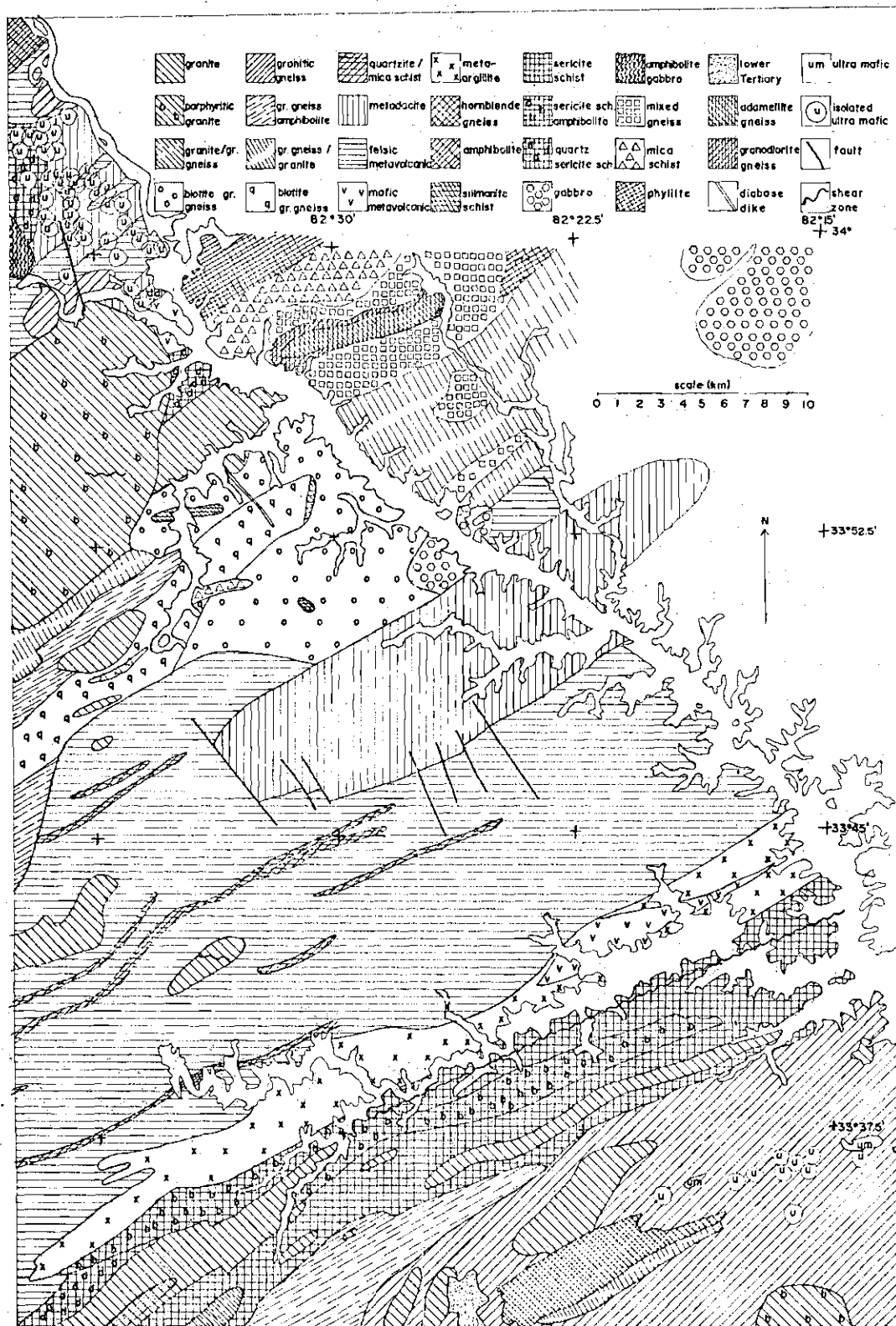


Figure 2. Geology Map of the Clark Hill Reservoir Area  
Geologic Map of Georgia, Georgia Geological Survey, 1976.

The travel time curve that Dorman determined yields a two layer velocity model. The top layer extends to a depth of 43 km and has a velocity of 6.2 km/sec. The second layer, which represents the Moho, has a velocity of 8.2 km/sec. The data for this model were obtained from the ATL Seismic Observatory records of several quarry blasts.

Guinn (1976) determined a travel time curve for the piedmont using data from the Preliminary Determination of Epicenters (U. S. Geological Survey) and the ATL records. His curve yields a three layer model. The top layer extends to a depth of 12.9 km and has a velocity of 5.57 km/sec. The second layer extends from 12.9 to 35.6 km and has a velocity of 6.33 km/sec. The third layer, which represents the Moho, starts at 35.6 km and has a velocity of 8.15 km/sec.

Previous work concerning local velocity measurements in the CHRA has been done by Denman (1974) and Leary *et al.* (1975). Denman's model was obtained from the S-P times of quarry explosions recorded in the southern part of the CHRA. The apparent S-P velocity obtained was 8.20 km/sec. It was assumed that the P-wave velocity to S-wave velocity ratio is the square root of three. This yields a P-wave velocity of 5.80 km/sec and an S-wave velocity of 3.55 km/sec. This model consists of a uniform half space.

Leary *et al.* (1975) arrived at two possible models. The first model consists of three layers. The top layer is

a 33 meter thick weathering zone with a P-wave velocity of 1.14 km/sec. The middle layer is 500 meters thick and has a P velocity of 5.92 km/sec. The bottom layer is a half space with a P velocity of 6.15 km/sec. The second model calls for a continuous small linear increase in velocity with depth.

### Seismic History of the Clark Hill Reservoir Area

The only earthquake known to have occurred in the CHRA prior to 1963 was the November 1, 1875 event of Modified Mercalli Intensity VI. Intensity data indicated an epicenter between Lincolnton and Washington, Georgia (Denman, 1974). Due to sparse population in the area, minor events probably would not have been reported.

In 1963 the ATL Seismic Observatory was installed near Lovejoy, Georgia. Between 1963 and 1975, over 50 events that are believed to have originated in the CHRA, with magnitudes of 1.8 or above, were recorded at ATL (Denman, 1974; Long, 1974).

On August 2, 1974 an earthquake of magnitude  $m=4.3$  (Earthquake Data Reports No. 62-74, U. S. Geological Survey) occurred in the northern part of the CHRA. This was followed by an earthquake swarm that lasted for several months (Bridges, 1975). There is, as yet, no clearly defined, generally agreed upon, fault or set of faults responsible for this activity. The possibility of multiple non-parallel faults is indicated by the earthquake locations

(Bridges, 1975) and spectral data (Marion, 1977) which are inconsistent with a single fault source.

The minimum detectable local magnitude was reduced to  $0.3 \pm 0.2$  in December 1975 with the installation of stations CH5 and CH6 near Double Branches and Goshen, Georgia. Since then several additional stations have been installed. Signals from these stations are recorded in Atlanta.

In addition to the aftershocks of the August 2 event west-southwest of Willington, recent activity has been observed in the southern part of the lake along Georgia's Little River (Denman, 1974), in the western part of Fishing Creek (1976), north of Hickory Knob State Park (1977) and southeast of Plum Branch, South Carolina (1976) (see Figure 3).





## CHAPTER 2

### Methods and Data

The seismic sources used were explosions set off for the construction of the diversion channel for the Richard B. Russell Dam. The size of the explosions ranged from several hundred to several thousand pounds of explosives.

The explosions were recorded by fixed and portable instruments. The fixed instruments were stations CH5, CH6 and RF1. These stations are part of the telemetered seismic monitoring system operated by the School of Geophysical Sciences, Georgia Institute of Technology, in the CHRA. Their signals were recorded in Atlanta. Events of sufficient amplitude were also recorded on magnetic tape for later use. Data from these stations were used to determine a relative travel time from the shots.

The portable instruments used were high frequency tape recorders and a Sprengnether MEQ-800. The characteristics of the tape recorders are described by Marion (1977).

The locations for the instruments were determined from 7 1/2" quad sheets. The error in the locations was of the order of six meters. Table 1 is a list of all stations (see Appendix A). Figure 4 is a map showing the locations of these stations. The stations form two refraction lines. The short line between the refraction lines did not yield

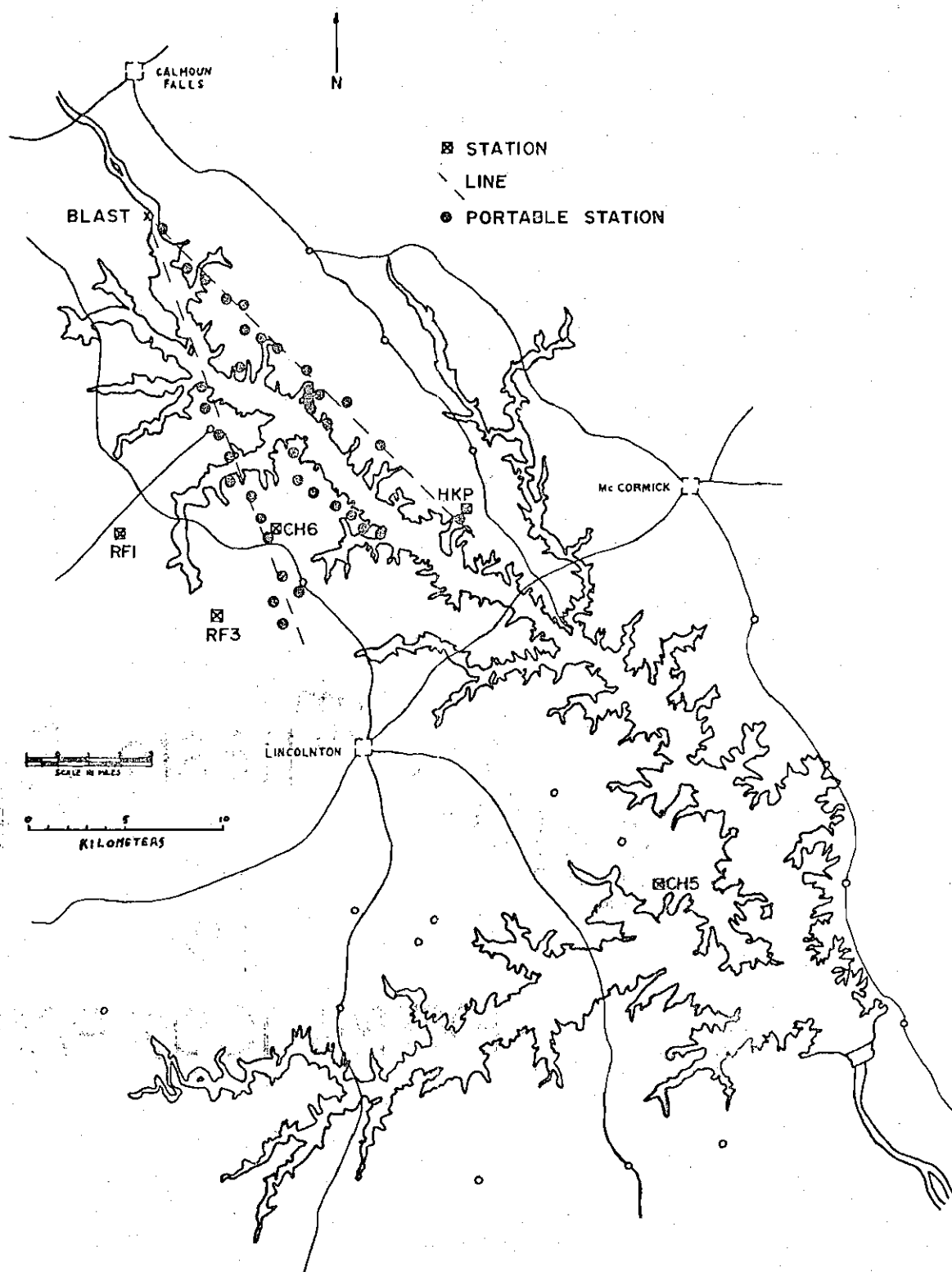


Figure 4. Map Showing Blast Site and Station Locations

enough data to be used as a third refraction line. The short line does serve to connect the two refraction lines.

The locations of the explosions are known only to within a rectangular area that is 0.5 km long by 0.1 km wide. However, most of the explosions took place in an area that is 0.25 km long by 0.1 km wide. The center of this area is taken to be the location of the explosions.

In order to combine the data from separate explosions, the explosions had to be recorded by both the portable stations and at least one of the permanent stations. Timing accuracy associated with the measurements was  $\pm 5$  msec for the permanent stations, provided the explosion was recorded on magnetic tape in Atlanta and the clock correction was known. Otherwise, an accuracy of  $\pm 0.3$  sec was assumed. The timing accuracy of the tape units was  $\pm 5$  msec if the WWV radio reception was good. The record was not used for first arrival times if the WWV reception was poor or nonexistent. The accuracy of the Sprengnether recorder was no better than  $\pm 0.02$  sec for absolute time. Relative times, such as S-P time, could be measured to  $\pm 0.01$  sec. Elevation differences between stations could cause arrival time deviations on the order of  $\pm 0.005$  sec. This number was computed by using the maximum elevation difference between a station with absolute time data and the average elevation of the stations. A near-surface velocity of 4.55 km/sec was also used. Errors due to the uncertainty in the blast position were on the order

of  $\pm 0.02$  sec. This was calculated by using the uncertainty in the blast position and a velocity of 6.1 km/sec. This velocity is approximately the slope of the travel time curve beyond 10 km.

Travel times were computed using an origin time 6.83 sec earlier than the first arrival at station CH5. This number was computed using CH5 and a station close to the blast site. The timing accuracy of the station was  $\pm 0.025$  sec. Its distance from the explosion was estimated to be 250 meters. No allowance was made for a surface layer so the 6.83 sec value is arbitrary. Table 2 is a list of travel times, reduced travel times and shot-station distances (see Appendix A).

Figure 5 is a reduced travel time plot for first arrivals at all stations with absolute time data. The reduced velocity used on all figures is 6.5 km/sec. The squares in the figures represent the permanent stations.

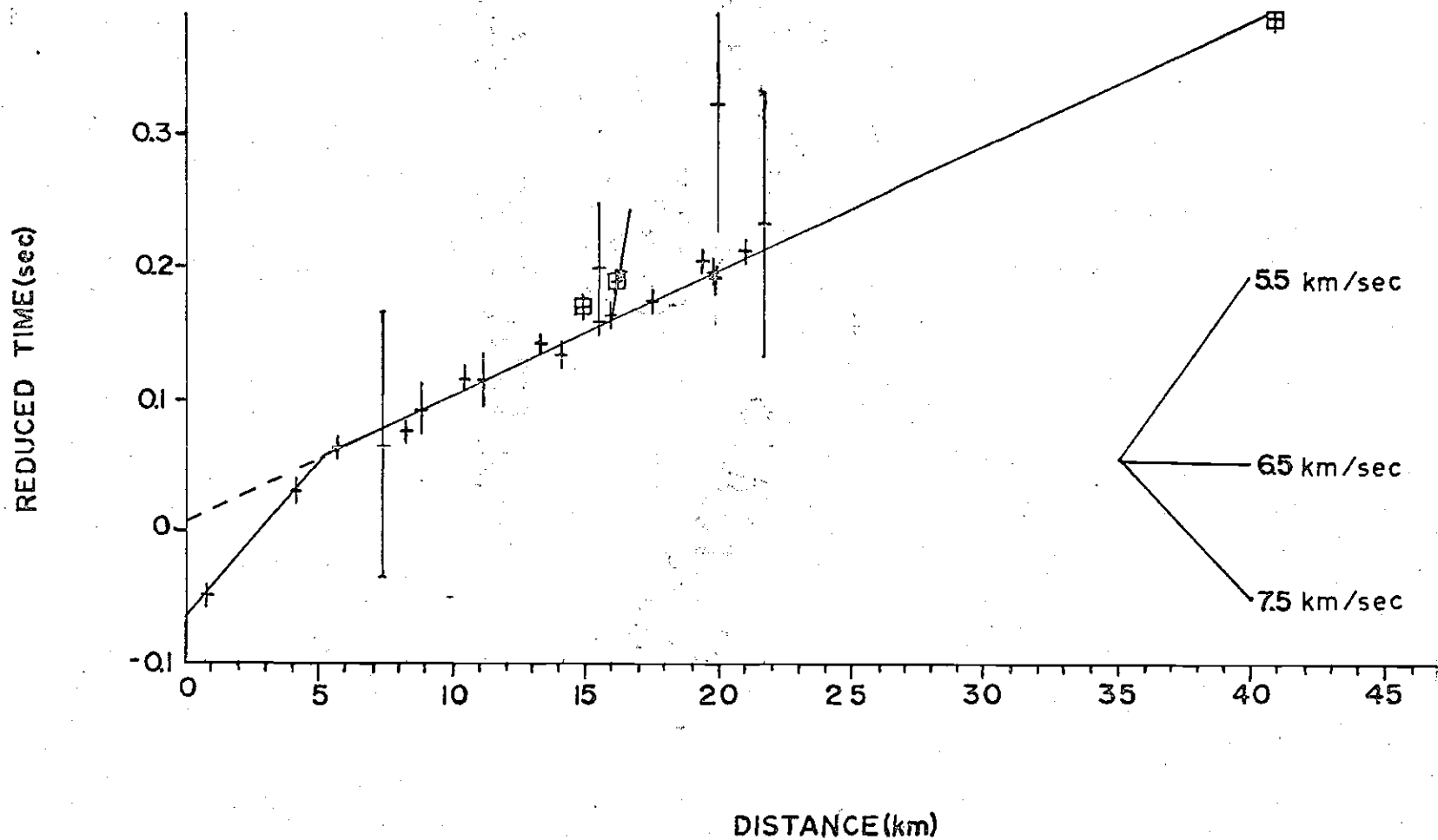


Figure 5. Plot of Reduced First Arrivals  
The reduced velocity used is 6.5 km/sec.

## CHAPTER 3

### Velocity Model

The new velocity model was developed by using a raytracing method. The travel time curves computed by the raytracing method were compared with the actual data and the model was modified to produce a better fit. Appendix B describes the computer program used for the computation.

The P-wave Velocity model that best satisfied the data is listed in Table 3. The velocity between the points listed is continuous and linear. Depth is measured from sea level. The raypath from the source to the most distant station used in this study penetrates to a depth of 3.37 km according to the model. Below this depth, the model comes from other sources (Dorman, 1972; Guinn, 1976) and is currently under revision. Figure 6 presents the model graphically.

The layer from -0.13 to 0.17 km represents the weathering zone. The velocity at the surface is poorly constrained. The layers from 0.17 to 5.0 km may represent a fairly normal increase in velocity with increasing pressure (Stewart and Peselnick, 1977). The reversal in the velocity at 5.0 km is partially an artifact of combining the Clark Hill model with Guinn's regional model for the Piedmont. However, the reversal does have some physical basis. There does appear to be a high-velocity near-surface channel. Arrivals at

Table 3. P-wave Velocity Model

Depth(km)    Velocity(km/sec)

-0.13            4.55

0.17            5.80

0.57            6.10

5.0            6.42

5.0            5.57

12.9            5.57

12.9            6.33

35.6            6.33

35.6            8.15



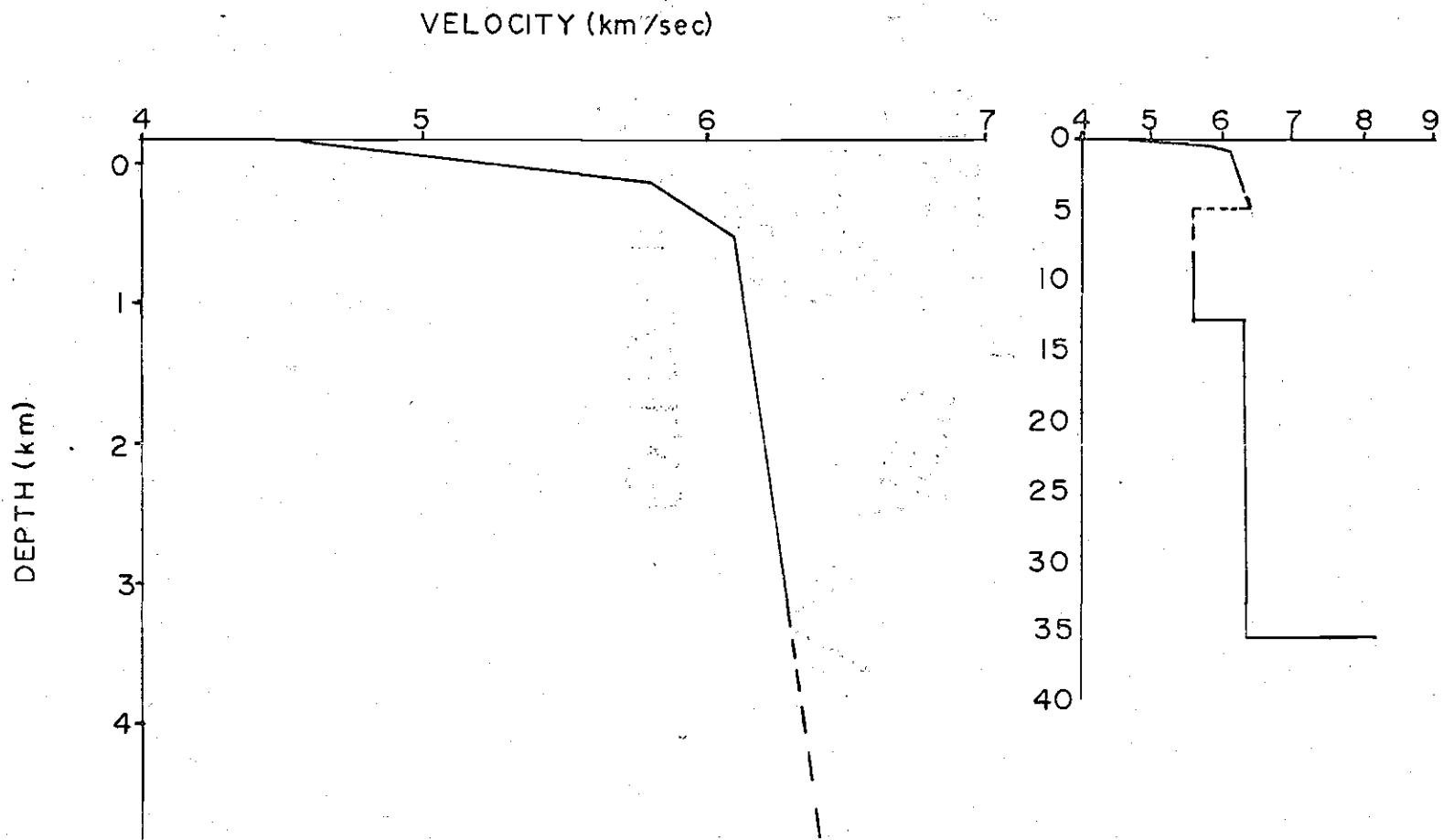


Figure 6. P-wave Velocity Model

The local model is on the left. The regional model is on the right.  
The regional model is under revision. The dashed line is conjectural.

stations more than a few kilometers from an event are quite complicated. A high-velocity channel explains this quite well as there would be many reflections within the channel. The depth of 5.0 km is arbitrary, but is of the proper order of magnitude to produce the observed effects. Lateral inhomogenities would also contribute to the complexity of arrivals.

Figure 7 is the theoretical reduced travel time curve for the region of interest. Comparison of Figures 5 and 7 indicates a good fit if the origin time used for the data reduction is shifted 0.08 sec earlier. This is not an unreasonable correction since no allowance was made for a surface layer.

The fit of the model with the travel time curve is surprisingly good considering the mix of rock types involved. At pressures experienced near the surface, granites have P-wave velocities of  $5.1 \pm 1.7$  km/sec, gneisses have velocities of  $4.3 \pm 1.4$  km/sec, schists have velocities of  $5.7 \pm 1.1$  km/sec, and gabbros have velocities of  $6.3 \pm 0.6$  km/sec (Birch, 1960). The seismic velocity of a rock increases with pressure. At a pressure of one kilobar, granites have velocities of  $6.2 \pm 0.4$  km/sec, gneisses have velocities of  $6.0 \pm 0.3$  km/sec, schists have velocities of  $6.4 \pm 0.4$  km/sec, and gabbros have velocities of  $7.0 \pm 0.2$  km/sec (Birch, 1960). The other rock types in the CHRA are expected to exhibit similar variability. The increase in velocity with pressure is

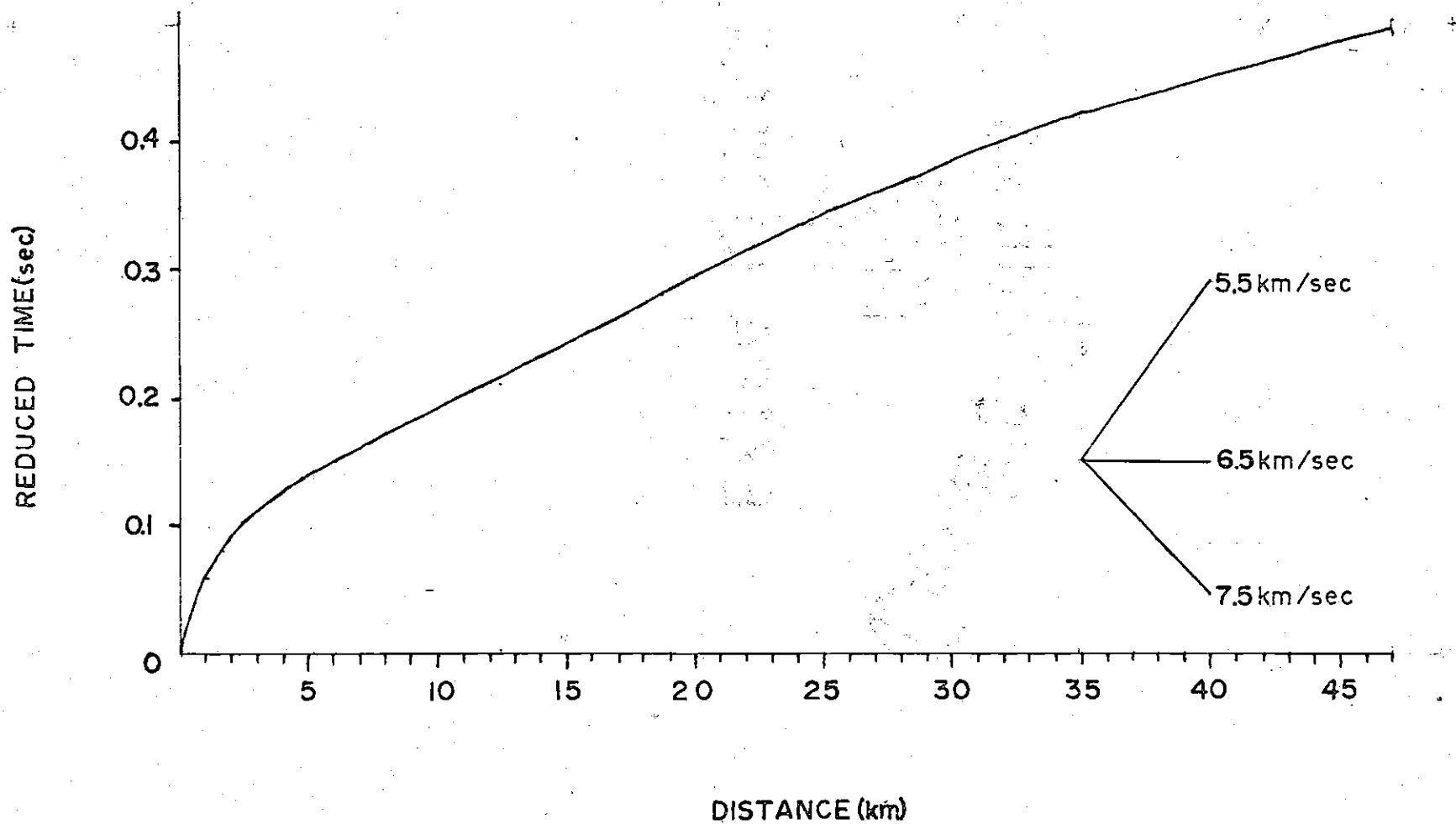


Figure 7. Theoretical Reduced Travel Time Curve

The reduced velocity used is 6.5 km/sec.

generally the most rapid as the pressure increases to one or two kilobars (Stewart and Peselnick, 1977).

Figures 8 and 9 are reduced travel time plots for stations on the Georgia and South Carolina refraction lines respectively. The geologic units the lines cross are indicated on these plots. The symbols for the rock types are the same as used on the geology map (Figure 2). Comparison of Figures 8 and 9 indicates that the velocity structure on each side of the lake is essentially identical. The lack of effect due to rock type is readily seen.

A separate S-wave model has not been developed. The reason behind this is the rather severe mismatch between the frequency content of the shear waves produced by the explosions and the frequency response of the tape units (Marion, 1977). Also the tape unit's records are generally characterized by multiple arrivals. As a result of this, it is almost impossible to distinguish a shear wave in the tape unit's record. Several stations did record clear shear wave arrivals. These indicate that the generally used approximation

$$V_s = V_p / \sqrt{3}$$

is good to within a few percent in this area. This approximation is based on a value of 0.25 for Poisson's ratio. This value is found to be applicable in most cases.

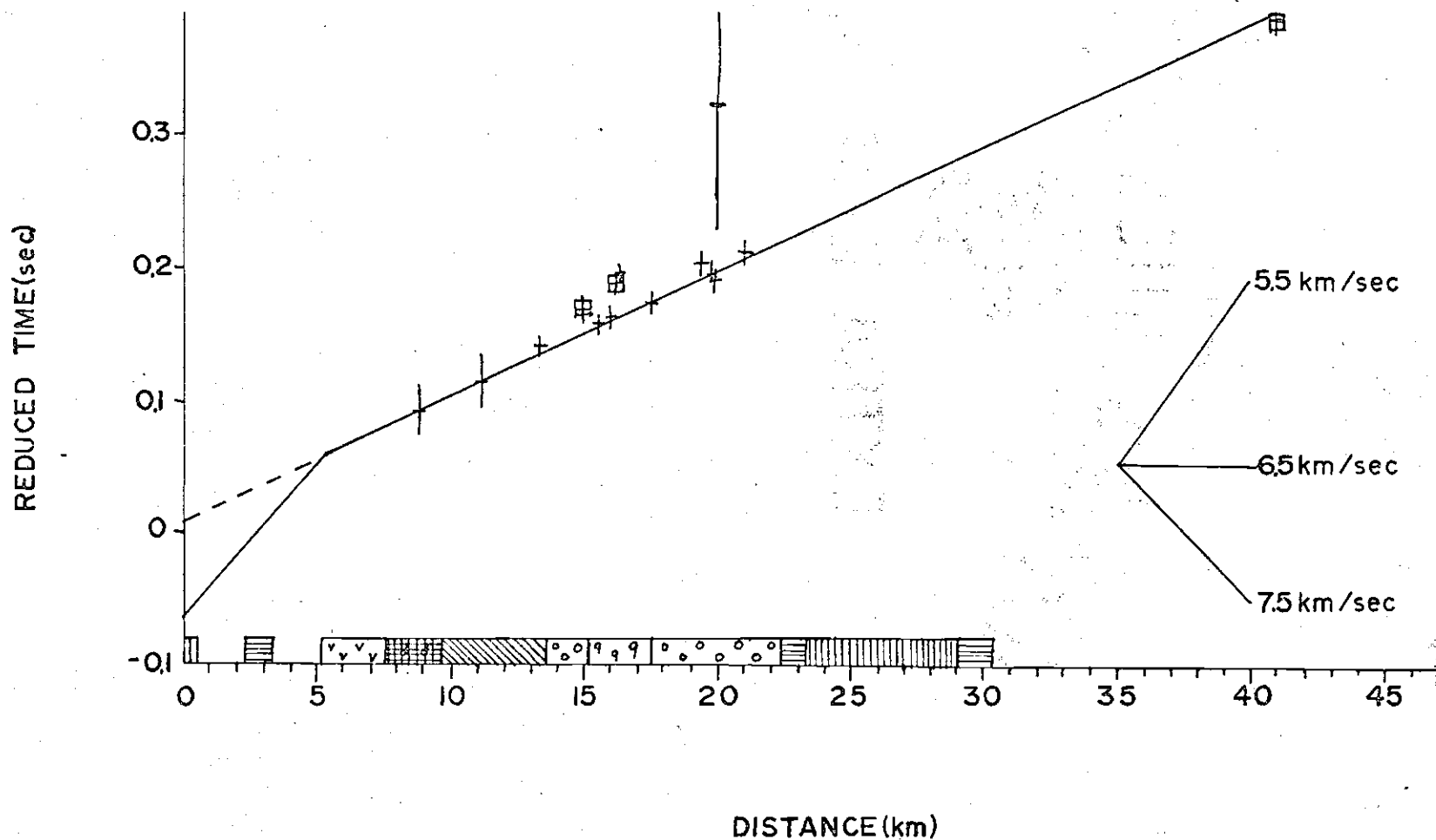


Figure 8. Reduced First Arrivals, Georgia Side

The reduced velocity used is 6.5 km/sec.

See Figure 2 for the geologic units.

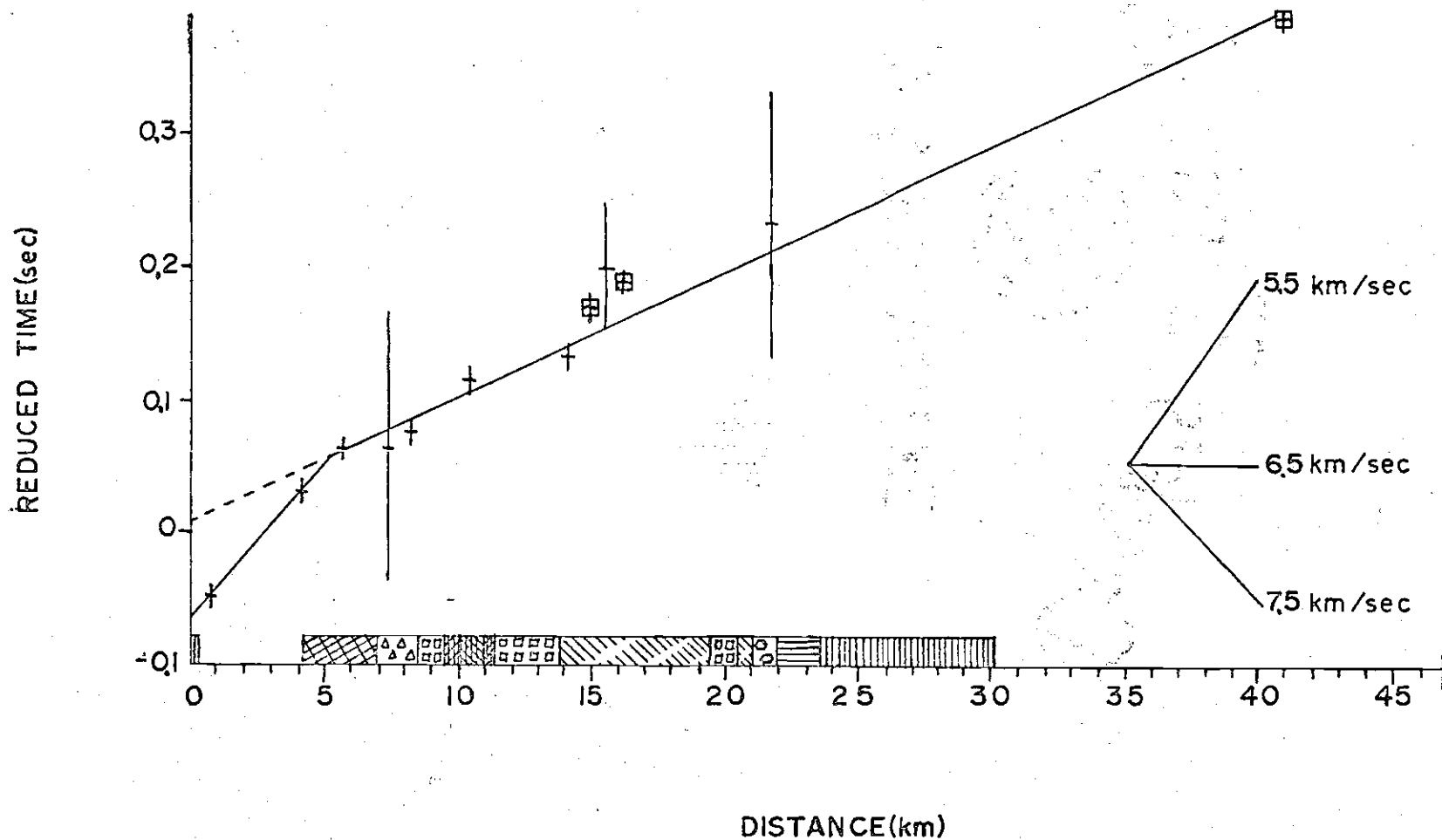


Figure 9. Reduced First Arrivals, South Carolina Side

The reduced velocity used is 6.5 km/sec.  
See Figure 2 for the geologic units.

Several stations also recorded Rayleigh waves. The velocity of these waves is  $3.0 \pm 0.3$  km/sec. Using the same value of Poisson's ratio and the 6.1 km/sec P-wave velocity used earlier, the surface wave velocity is computed to be 3.2 km/sec (Garland, 1971).

Figure 10 is a comparison of the new model, Denman's model and the first model of Leary et al. As can be seen, the most significant differences between the models occur at shallow depths. The new model gives longer travel times for the range of depths in which earthquakes have been recorded (see Appendix D).

#### Relation to Geology

The only significant deviations from the velocity model occur in the vicinity of stations CH6, RF1 and HKP. The deviation near CH6 occurs in the middle of a rock unit identified on the Geologic Map of Georgia as an epidote quartzite/granite gneiss. The stations in this unit are ST1, ST2, ST3 and CH6. There are no significant deviations at stations ST2 and ST3. Arrivals at stations ST1 and CH6 are delayed by 0.020 to 0.025 sec compared to the travel time curve. These stations were occupied at the same time so differences in shot locations is not a factor. Elevation differences between the stations are slight and can not explain the delay. The apparent P-wave velocity in the unit is  $4.1 \pm 0.5$  km/sec.

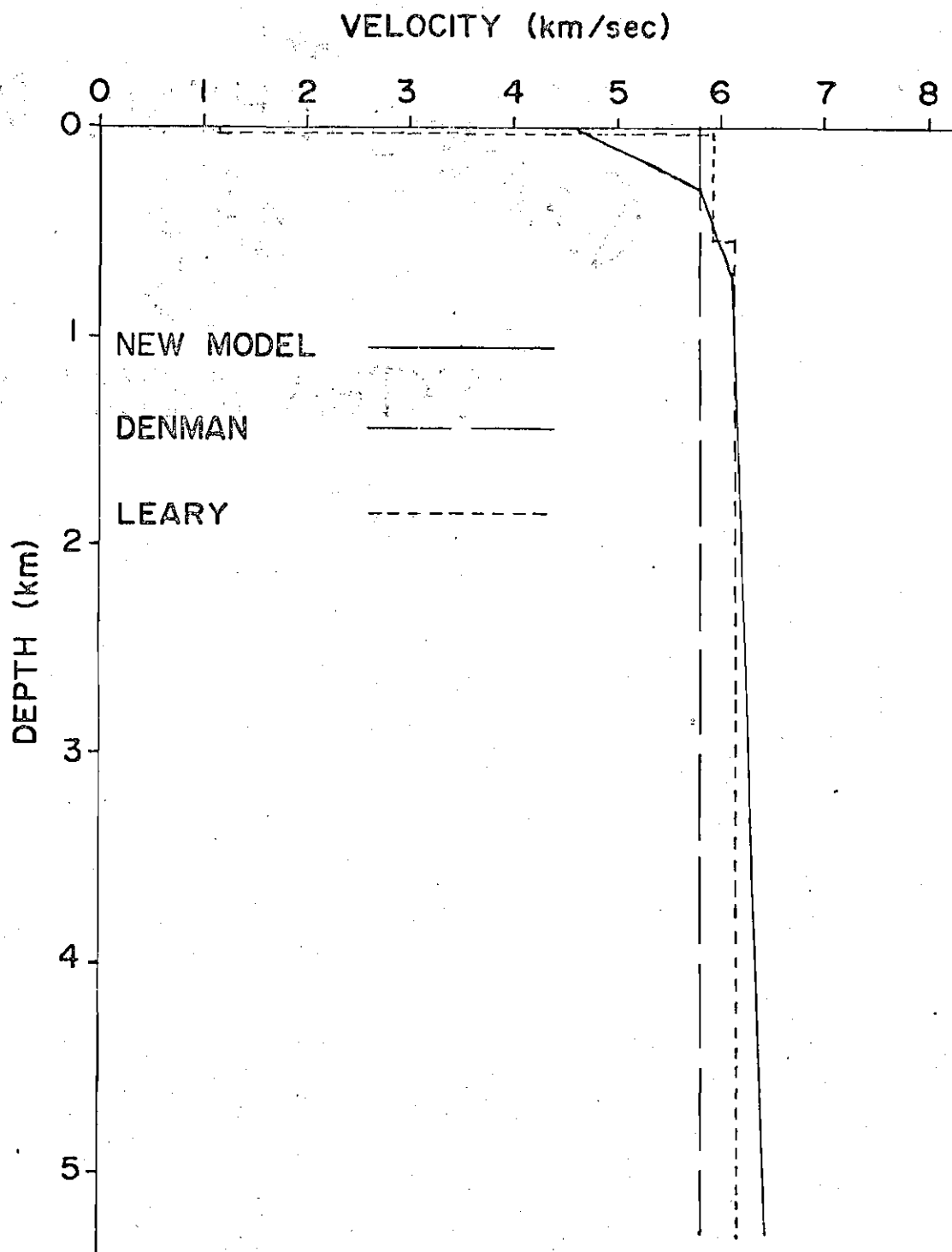


Figure 10. Comparison of Velocity Models



Some structure within the unit is indicated. The unit is apparently fairly thin under ST2 and ST3; on the order of 100 meters or less. It thickens to something on the order of 300 meters under ST1 and CH6. The thickening takes place fairly abruptly since ST1 and ST2 are less than 0.5 km apart. These thicknesses were calculated by assuming that the delay is due to material that has a velocity of 4.1 km/sec. The 100 meter thickness would produce a delay of less than 0.01 sec, which is the limit of detection. The 300 meter thickness would produce the observed delay. The nature of the thickening is not readily apparent. It could be due to a fault or folding of the unit. In either case, the unit does not extend to great depths since the next station on the refraction line, GS2, does not show a significant delay.

The Danburg granite also has a velocity anomaly. The only station in this unit, RF1, has a first arrival that is delayed by 0.017 sec. This yields an apparent velocity of 6.04 km/sec. This number may be subject to revision since there were no other stations in this unit and RF1 is off the refraction lines. The apparent velocity was calculated by assuming that the travel time curve is unaffected until the seismic ray enters the Danburg granite. The delay was assigned to the portion of the raypath that passes through the granite.

Another velocity anomaly is reported in the preliminary report by Leary et al. (1975). The study shows

a high velocity unit in the vicinity of Hickory Knob State Park. The rock in and around the park is a gabbro. The velocity was found to be 6.21 km/sec in this area.

The apparent velocity for some of the rock units has been calculated by taking the differences in travel time to different stations in the units. On the Georgia side of the lake, the granite unit has an apparent velocity of  $6.08 \pm 1.04$  km/sec. The biotite granite gneiss, labeled "o" on the geology map, has an apparent velocity of  $6.11 \pm 0.66$  km/sec.

On the South Carolina side, no single unit has enough stations with absolute time to determine the velocity through the unit. The sequence of rock units from the phyllite through the adamellite gneiss has an apparent velocity of  $6.06 \pm 0.51$  km/sec. The sequence from the adamellite gneiss through the granite gneiss/granite has an apparent velocity of  $6.31 \pm 0.64$  km/sec.

The combination of the regional velocity model with the revised near-surface model suggests that the structure of the CHRA could be described as a high-velocity layer with pods of lower velocity material in it. These pods may be shallow or they may extend to considerable depths. The rock unit responsible for the anomaly at station CH6 is apparently quite shallow. The vertical extent of the rock units responsible for the other two anomalies can not be delimited by the data.

The velocity structure in the northwestern half of

the CHRA is remarkably uniform laterally. The anomalous rock units that are present are fairly limited in extent. Other anomalies may be present, since the current study is not sensitive enough to distinguish anomalies that produce travel time variations of less than 0.01 sec.

## CHAPTER 4

### Comparison of Earthquake Locations

Appendix D gives a listing of locations of earthquake foci, as determined by both Denman's model and the revised model. These show significant differences in latitudes and longitudes. The relocated epicenters are an average of 105 meters from the old epicenters. The depths of focus also differ, the revised model generally gives shallower locations, by an average of 140 meters. An unexpected result of the new velocity model is that the earthquake location program will not converge for very shallow events. The reason for this is shown in Figure 11, which is a plot of travel times at short distances for events occurring at different depths. As the figure shows the curve for a near-surface focus crosses the curves for other depths. The effect is of the most importance for shallow events. The result of this condition is that in order to determine a shallow event's depth, a station that is quite close to the epicenter is required. Otherwise the depth sequence option of the Locate program must be used. The Locate program is a modification of the Doall program (Bridges, 1975) and is used for earthquake location (see Appendix C).

Figure 12 is a plot of the relocated events listed in Appendix D. The origin of this plot is 33 degrees 57.5 min

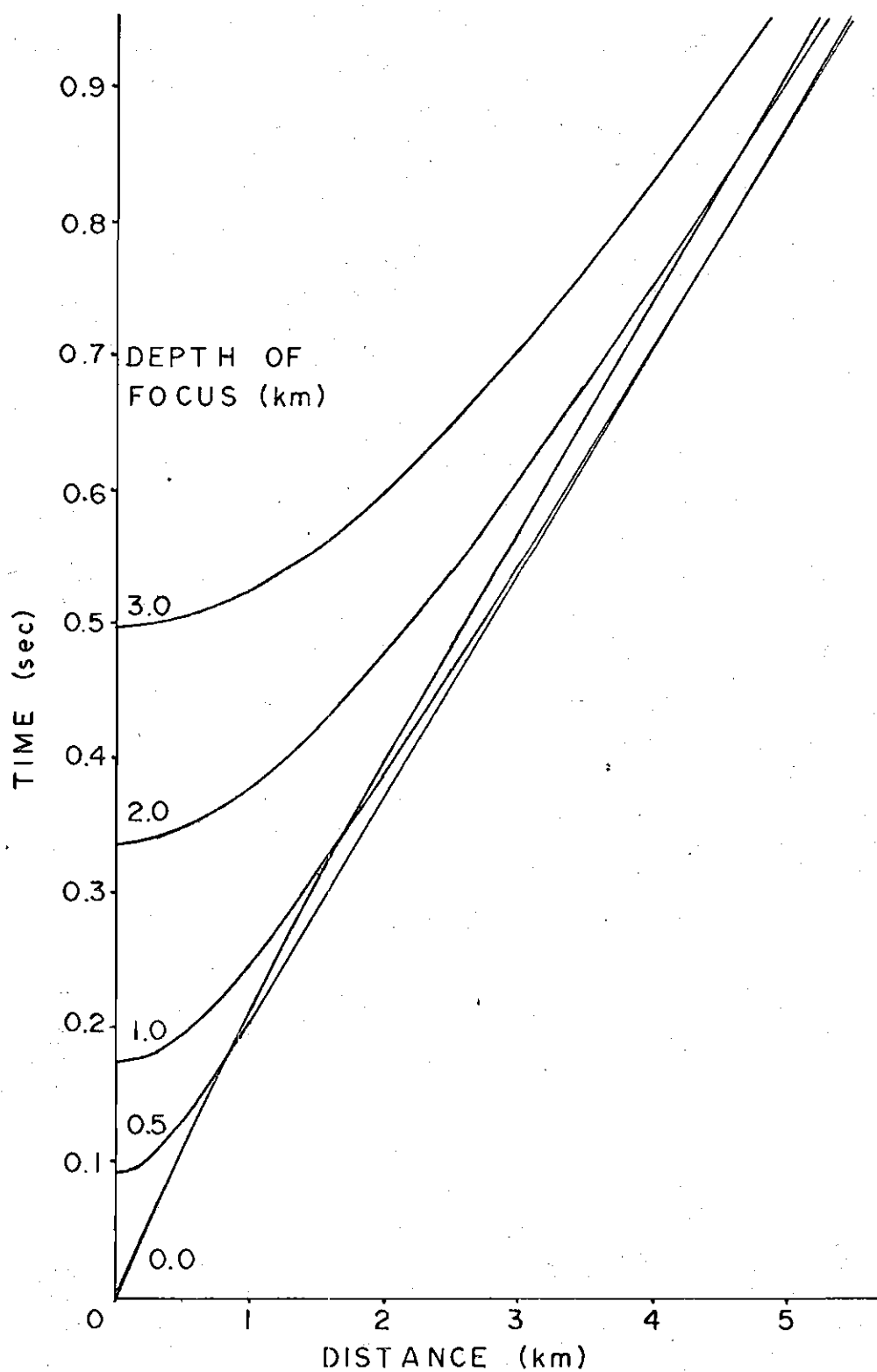


Figure 11. Plot of Travel Time Curves for Increasing Depths

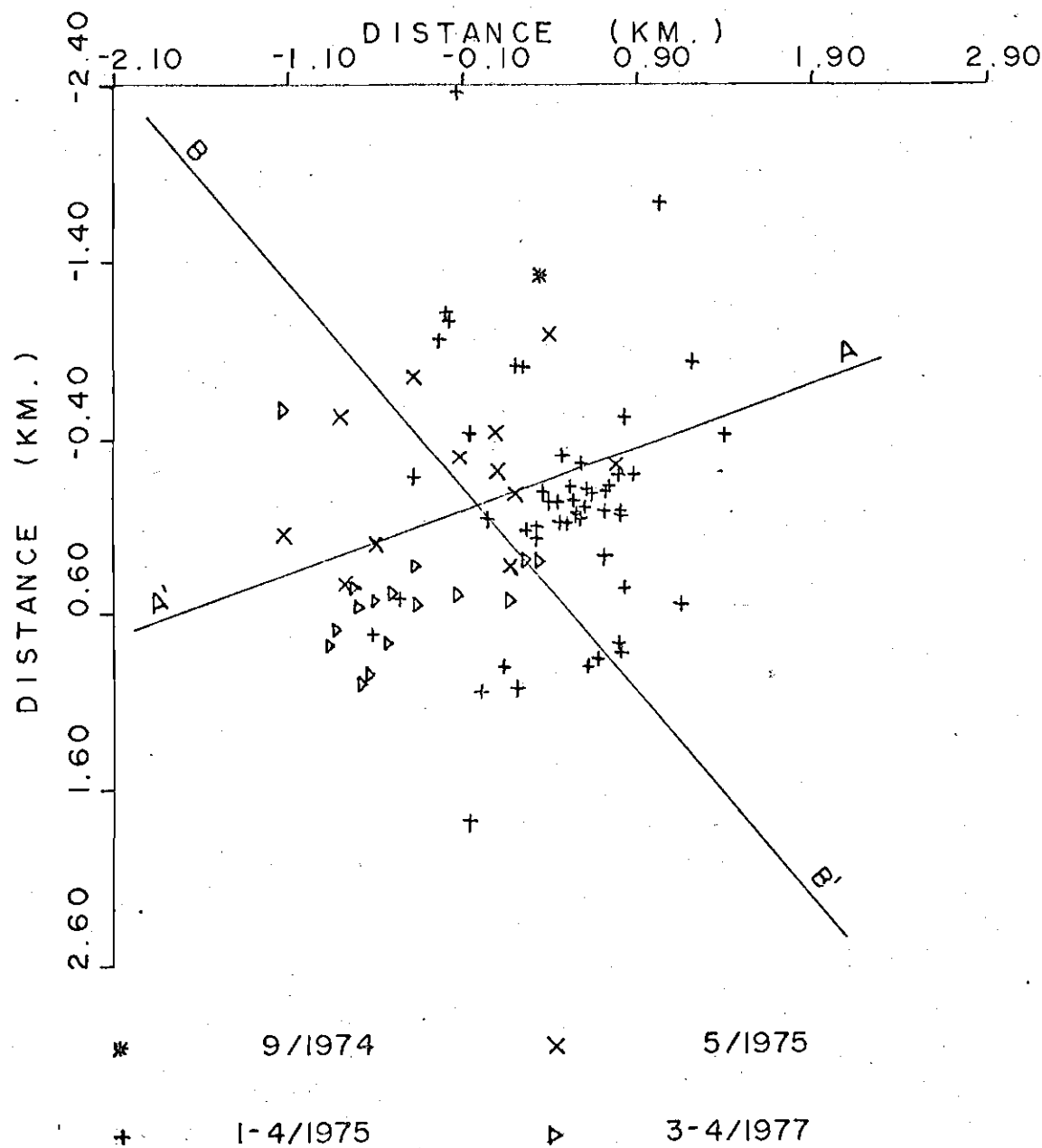


Figure 12. Plot of Relocated Epicenters

north and 82 degrees 30.0 min west. The different symbols correspond to events occurring on different dates. As can be seen, the events are not randomly distributed. Several features are visible in the plot. Possible faults are indicated by linear features.

In an effort to determine a quantitative measure of the randomness of the epicenters, the plot was contoured for the number of events in a 2.54 cm square (2.54 cm corresponds to 0.8 km). There is an average of 3.9 events per square. The resulting distribution of events per square was compared with both the normal and Poisson distributions by the use of the chi-squared test. For the normal distribution, the value for the test is 98. For the Poisson distribution, the test diverged. Both results indicate that the distribution of earthquakes is not random.

Figure 13 is a plot of epicenters as determined by Denman's model. The symbols are the same as in Figure 12. On the scale of the plots, comparatively little can be said about the relative merits of the two velocity models. Figure 13 does show more scatter in the epicenters than Figure 12 does.

The earthquake foci were projected onto various vertical planes orientated about the vertical axis. The projections were examined for linear trends.

Figure 14 is projection A'-A. In this figure, the earthquakes have been projected onto a plane striking N 70 E.

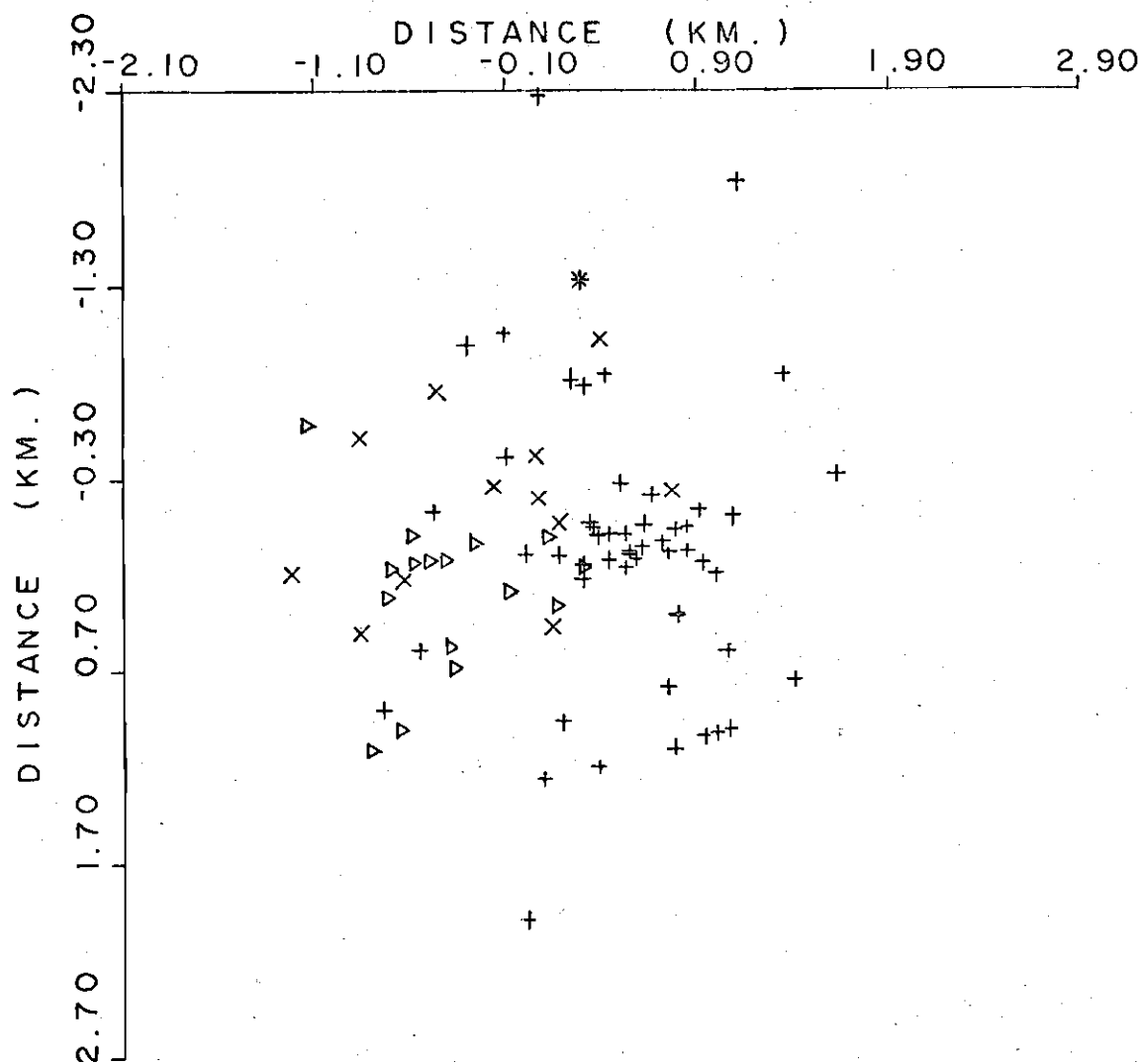


Figure 13. Plot of Epicenters as Determined by  
Denman's Model



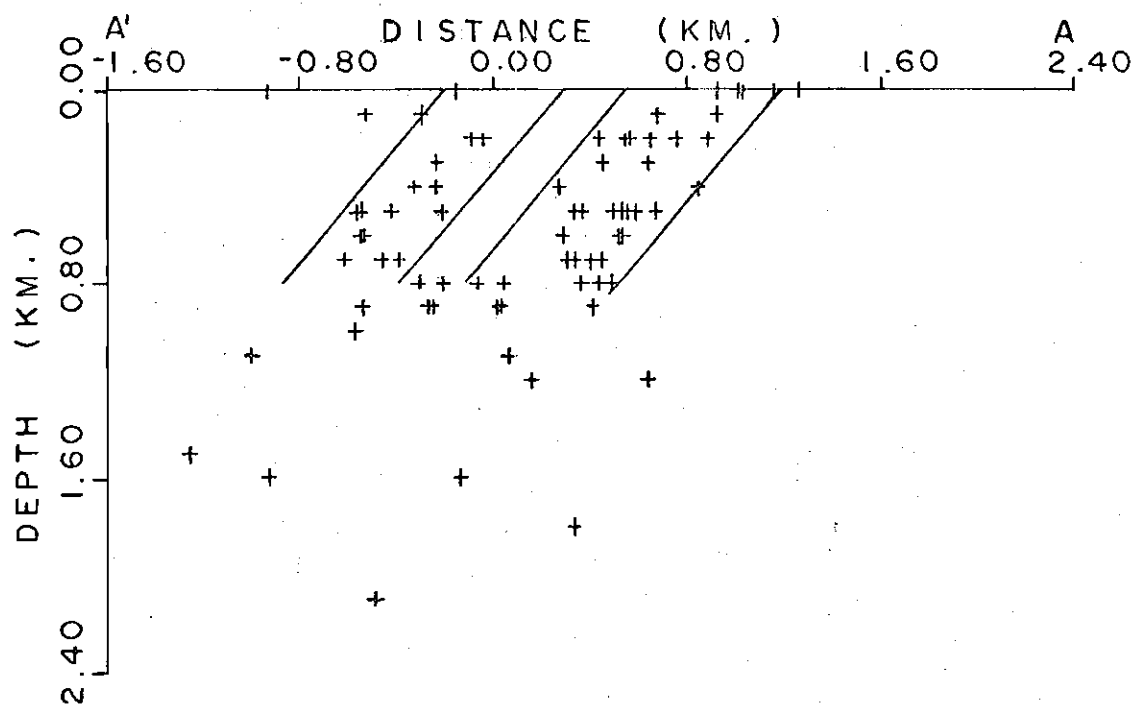


Figure 14. Projection A'-A

See Figure 12. The positive end  
of the distance axis is N 70 E.

The figure suggests two shallow zones of activity that strike approximately N 20 W and dip approximately 50 SW. There is a joint system roughly parallel to these zones (Guinn, 1977). The connection between the joint system and the zones, if any, is not clear. Joint systems are abundant in this area.

Figure 15 is projection B°-B. In this figure, the earthquakes have been projected onto a plane striking N 40 W. The figure suggests a planar structure whose orientation is N 50 E, 57 NW. There is some topographic expression of this feature. It is approximately paralleled by two small valleys. An extension of the plane across the lake approximately coincides with the northeast trending part of Fishing Creek (see the Chenault and Willington quadrangle sheets). No activity has been located in this part of Fishing Creek.

Of the 81 relocated earthquakes (see Appendix D), 39 are within 200 meters of the median plane of the B°-B structure. The 39 events were removed from the data and the remainder were projected onto various planes in a search for other linear trends. No such trends could definitely be identified; however, there are indications of several linear trends.

#### Conclusions, Comments and Recommendations

If this study is ever expanded, there are a number of recommendations. The first is to have better control of the

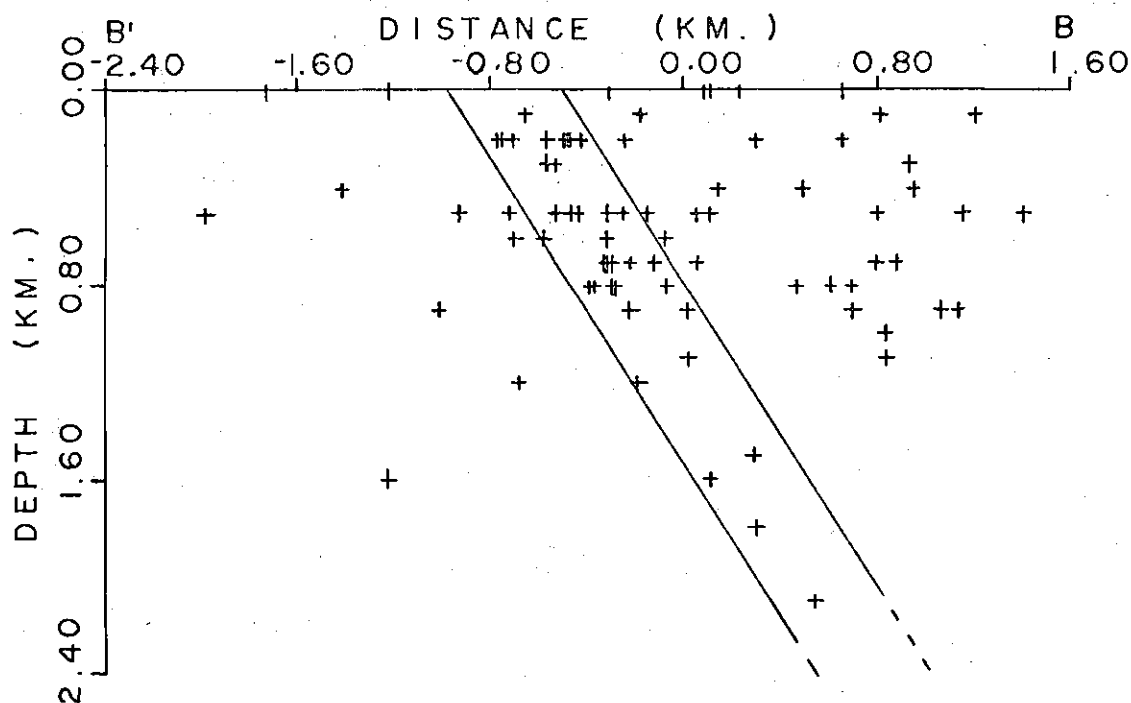


Figure 15. Projection B'-B

See Figure 12. The positive end of the distance axis is N 40 W.

blast locations and shot times. This problem is the biggest single source of error in the present study. The preferred method used for refraction work calls for the ability to determine shot and arrival times to an accuracy of  $\pm 1$  msec or better, weathering corrections, and shot-geophone distances to an accuracy of  $\pm 1$  meter or better. In the present study, none of these could be done.

The easiest way to improve the accuracy of subsequent studies is to place an expendable geophone as close as possible to the quarry blast to provide the origin time. There are a number of quarries in the CHRA that could be used as seismic sources.

The second recommendation is to run a reverse refraction line. The report by Leary *et al.* (1975) indicates that the velocity layers may be dipping.

The third recommendation is to add some sort of internal clock to the tape units. A considerable amount of data has been lost because the WWV radio reception was bad.

A few conclusions can be stated at this point. The first is that the CHRA has a near-surface high-velocity seismic channel. The overall dimensions of the channel are unknown. The job of delimiting these dimensions is left to later workers.

The second conclusion is based on the relocated earthquake foci. The plots of the foci show that the activity is not due to a single fault. The existence of at

least one fault or multiple fault is strongly suggested by the foci data. The 81 relocated events are only a small fraction of the events available for use. The Herculean task of relocating all of the available events is left to later workers.

It should be pointed out that the revised velocity model is an average representation of the velocity structure in the CHRA. The accuracy of the data and the irregularity of the geologic units will mask velocity anomalies that produce travel time variations of 0.01 sec or less.

The desirability of using a local velocity model for earthquake location in regions with significant velocity inhomogeneities has been demonstrated (Aki and Lee, 1976). The purpose of using a local model is to obtain earthquake foci that are as close as possible to the actual locations of the earthquakes. If the velocity structure of an area is unknown or poorly known, almost any model can be used to obtain approximate locations. A local model is required if a study is undertaken to identify the location and orientation of a fault or to decide which of several faults are active. In the present study, the use of a local model has significantly reduced the scatter of the earthquake foci.

## APPENDIX A.

Table 1. Locations of Stations

Station	Latitude(N)	Longitude(W)	Elevation(km)
CH5	33.7332	82.3118	0.1143
CH6	33.8395	82.5289	0.1463
RF1	33.8920	82.6111	0.1509
RF2	33.9412	82.4781	0.1768
RF3	33.8280	82.5107	0.1530
HKP	33.8943	82.4227	0.1554
HRC	33.9478	82.4770	0.1582
466	33.9590	82.5189	0.1420
CFP	34.0206	82.5930	0.1247
BMS	34.0046	82.5758	0.1161
ST1	33.8696	82.5320	0.1478
ST2	33.8920	82.5355	0.1372
ST3	33.8955	82.5384	0.1414
SID	33.9867	82.5443	0.1524
MPB	33.9983	82.5672	0.1035
YST	33.9898	82.5548	0.1448
PPP	33.9746	82.5474	0.1469
LCC	33.9709	82.5374	0.1341
MTC	33.9661	82.5310	0.1082
ACF	33.9520	82.5088	0.1067
PTT	33.9491	82.5110	0.1067

Table 1. Continued

GNC	33.9452	82.5106	0.1128
CUP	33.9431	82.5100	0.1067
SBS	33.9358	82.5023	0.1036
TOH	33.9499	82.5019	0.1539
MUD	33.9210	82.5186	0.1128
NOH	33.9110	82.5158	0.1372
HON	33.9048	82.5072	0.1402
ALS	33.8992	82.4975	0.1234
JPT	33.8973	82.4886	0.1189
POT	33.8915	82.4807	0.1082
ROT	33.8845	82.4691	0.1067
EOR	33.9119	82.5547	0.1036
GBR	33.9164	82.5554	0.1082
DRG	33.9298	82.5643	0.1021
EOC	33.9410	82.5696	0.1234
MGS	33.9498	82.5694	0.1189
TIR	33.9341	82.4706	0.1561
OTH	33.8930	82.4250	0.1161
CHG	33.8458	82.5323	0.1585
GSS	33.8573	82.5306	0.1433
GS2	33.8641	82.5229	0.1347
JAN	33.8600	82.5146	0.1247

Table 2. Reduced Data

Station	Travel Time(sec)	Reduced Time(sec)	Distance (km)
CFP	0.07	-.047	0.76
MPB	0.67	.028	4.18
YST	0.93	.062	5.64
PPP	1.197	.064	7.37
LCC	1.347	.074	8.28
MGS	1.463	.095	8.89
466	1.715	.114	10.41
DRG	1.829	.115	11.15
GBR	1.795	-.176	12.81
EOR	2.188	.140	13.31
HRC	2.305	.133	14.12
RF1	2.475	.169	14.99
ST3	2.545	.158	15.52
TIR	2.59	.200	15.54
ST2	2.620	.162	15.97
ST1	2.710	.196	16.34
CH6	2.685	.188	16.46
JPT	2.865	.174	17.49
GS2	3.170	.204	19.28
ROT	3.225	.195	19.70
GSS	3.230	.191	19.76
JAN	3.400	.325	19.93



Table 2. Continued

CHG	3.430	.211	20.93
OTH	3.565	.233	21.73
CH5	6.833	.389	41.87

## APPENDIX B.

### Travel Program

The program Raypath was developed by L. T. Long to compute travel times, reduced travel times, distances and amplitudes for phase arrivals from given flat-layered velocity models. The amplitude and reduced travel time parts of the program were removed when Raypath was converted to a subroutine for the program Travel.

The program Travel computes interpolated travel times at 0.1 km steps from the input velocity model. The model used should have an extremely high velocity layer as the deepest layer in the model so close-in arrivals will be computed.

```

PROGRAM MAIN(INPUT,OUTPUT,TAPE5=INPUT,TAPE6=OUTPUT)
DIMENSION X(500),T(500),TC(40,251),DOF(40),NA(40)
DIMENSION VM(250),Z(100),V(100),ZZ(100),ZZZ(100),VV(100)
READ(5,*)NNA,NM
WRITE(6,300)NNA,NM
300 FORMAT(1X,"NNA =",I4,"M =",I4)
READ(5,*)(VM(I),I=1,NM)
C VM-THE MAXIMUM VELOCITY ENCOUNTERED ALONG A RAY
WRITE(6,301)(VM(I),I=1,NM)
301 FORMAT(1X,"VM ARRAY",/,20(1X,10F8.4,/))
READ(5,*)(Z(I),V(I),I=1,NNA)
C Z AND V-THE DEPTH AND VELOCITY OF POINTS IN THE MODEL
WRITE(6,134)(Z(I),V(I),I=1,NNA)
READ(5,*)NDOF,(DOF(I),I=1,NDOF)
C DOF-THE DEPTHS OF FOCUS FOR THE SEISMIC SOURCES
C EACH DOF SHOULD EQUAL SOME Z
134 FORMAT(1X," DEPTH VELOCITY",/,2(1X,F10.3))
READ(5,*)NPD,(ZZ(I),I=1,NPD)
C ZZ-THE DEPTHS OF THE BREAKS IN THE VELOCITY MODEL
C THE ARRAYS VM,Z,DOF,AND ZZ MUST BE ARRANGED IN
C INCREASING ORDER
DO 150 I=1,NDOF
DO 190 J=1,NPD
DO 191 II=1,NNA
IF(Z(II).EQ.ZZ(J))VV(J)=V(II)
191 CONTINUE
190 ZZZ(J)=ZZ(J)
NPE=NPD
DO 20 J=1,500
X(J)=0.000000
20 T(J)=0.000000
DO 200 J=1,NPD
IF(DOF(I).EQ.ZZ(J))GO TO 203
200 IF(DOF(I).GT.ZZ(J).AND.DOF(I).LT.ZZ(J+1))GO TO 201
GO TO 203
201 NPE=NPD+1
NPF=NPE-J-1
DO 202 MM=1,NPF
ZZZ(NPE-MM+1)=ZZZ(NPE-MM)
202 VV(NPE-MM+1)=VV(NPE-MM)
ZZZ(J+1)=Z(I)
VV(J+1)=V(I)
203 CALL RAYPATH(X,T,VM,ZZZ,VV,NM,NPE,DOF(I))
NN=NA(I)=2*NM
J=0
31 J=J+1
IF(J.GT.NA(I))GO TO 30
IF(X(J).GE.0.001)GO TO 31
IF(T(J).GE.0.001)GO TO 31
N=NA(I)
DO 33 M=J,N

```

```

X(M)=X(M+1)
33 T(M)=T(M+1)
NA(I)=NA(I)-1
J=J-1
IF(J.LT.0)J=0
GO TO 31
30 CONTINUE
NN=NA(I) $J=1
8 NA(I)=NN
J=J+1
IF(J.GT.NN)GO TO 1
IF(X(J).GT.25.0)GO TO 4
IF(X(J)-X(J-1))3,4,8
3 JN=J-1
DO 5 M=1,JN
IF(X(J)-X(M))9,4,5
5 CONTINUE
9 JMM=J-M
XA=X(J) STA=T(J)
DO 7 N=1,JMM
X(J-N+1)=X(J-N)
7 T(J-N+1)=T(J-N)
X(M)=XA
T(M)=TA
GO TO 8
4 NN=NN-1
DO 10 M=J,NN
X(M)=X(M+1)
10 T(M)=T(M+1)
J=J-1
IF(J.EQ.1)J=2
GO TO 8
1 CONTINUE
WRITE(6,50)X(1),X(2),NA(I)
50 FORMAT(1X,/,1X,2F7.4,1X,I4,/)
AI=0.0
IF(X(1).EQ.0.0)TC(I,1)=T(1)
IF(X(1).EQ.0.0)GO TO 101
A=(T(1)-T(2))/(X(1)-X(2))
TC(I,1)=T(1)-A*X(1)
101 J=1
N=2
IF(X(1).GT.0.1)GO TO 103
105 AI=AI+0.1
104 IF(AI.GE.20.0)GO TO 100
IF(AI.GE.X(J).AND.AI.LE.X(J+1))GO TO 102
J=J+1
IF(J.GE.NA(I))GO TO 100
GO TO 104
102 A=(T(J)-T(J+1))/(X(J)-X(J+1))
TC(I,N)=A*AI+T(J)-A*X(J)

```

```

      N=N+1
      GO TO 105
103  A=(T(1)-T(2))/(X(1)-X(2))
106  AI=AI+0.1
      TC(I,N)=A*AI+T(1)-A*X(1)
      N=N+1
      IF(X(1).GT.(AI+0.1))GO TO 106
      GO TO 105
100  CONTINUE
150  WRITE(6,151)DOF(I),(TC(I,J),J=1,200)
151  FORMAT(1X,"DEPTH =",1X,F3.1,/,20(10(1X,F8.5),/))
      STOP
      END
      SUBROUTINE RAYPATH(XC,TC,VM,Z,V,NH,NN,DOF)
      DIMENSION V(100),Z(100),VM(250),XC(500),TC(500)
      WRITE(6,134)(Z(I),V(I),I=1,NN)
134  FORMAT(1X,"      DEPTH  VELOCITY",/,2(1X,F10.3))
      DO 210 I=1,NN
      IF(DOF-Z(I))211,211,210
210  CONTINUE
211  VDOF=V(I)
      DO 212 I=1,NH
      IF(VDOF-VM(I))213,213,212
212  CONTINUE
213  NMIN=I
      DO 130 I=NMIN,NH
      DESIG=1.0 $X=0.0 $T=0.0 $S=0.0 $NA=NN-1
      DO 125 J=1,NA
      IF(Z(J+1)-Z(J))17,125,110
17  WRITE(6,18)
18  FORMAT(1X,"INPUT ERROR")
      STOP
110  IF(Z(J)-DOF)207,202,202
202  SIG=2.0
201  IF(DESIG-SIG)206,207,206
206  XC(2*I-1)=X
      TC(2*I-1)=T
      IF(VM(I).GT.6.46)GO TO 130
      DESIG=SIG
207  IF(VM(I)-V(J))300,300,111
111  IF(VM(I)-V(J+1))126,126,112
112  IF(V(J)-V(J+1))113,114,113
113  AK=(V(J+1)-V(J))/(Z(J+1)-Z(J))
      AI1=ASIN(V(J)/VM(I))
      AI2=ASIN(V(J+1)/VM(I))
      S=S+DESIG*VM(I)*(AI2-AI1)/AK
      X1=VM(I)*COS(AI1)/AK
      X2=VM(I)*COS(AI2)/AK
      X=X+DESIG*(X1-X2)
      DT=(ALOG((AK*X1+VM(I))/V(J))-ALOG((AK*X2+VM(I))/V(J+1)))
      C/AK

```

```
T=T+DESIG*DT
GO TO 125
114 AI=ASIN(V(J)/VM(I))
DS=(Z(J+1)-Z(J))/COS(AI)
S=S+DESIG*DS
X=X+DESIG*DS*V(J)/VM(I)
T=T+DESIG*DS/V(J)
125 CONTINUE
126 CONTINUE
AK=(V(J+1)-V(J))/(Z(J+1)-Z(J))
S=S+DESIG*(VM(I)/AK)*(ACOS(V(J)/VM(I)))
X2=(VM(I)/AK)*SQRT(1.0-(V(J)*V(J))/(VM(I)*VM(I)))
X=X+DESIG*X2
DT=ALOG((AK*X2+VM(I))/V(J))/AK
T=T+DESIG*DT
300 XC(2*I)=X
TC(2*I)=T
130 CONTINUE
RETURN
END
```

## APPENDIX C.

### Locate Program

The Doall program (Bridges, 1975) has been modified for use as an interactive program. Most of the changes were made for ease of use. Options include the depth sequence which allows one to step the estimated focus through increasing depths to see where the best fit is. This option is used primarily for events that have occurred at shallow depths where the travel time curves give unstable results. Other options are used to input, extract or modify station, phase or arrival time information.

The Clark Hill travel time curves are read in from a file external to the program. The curves were computed for every 0.1 km increment in depth starting at the surface and going to 3.5 km. The numbers read in are the travel times interpolated at 0.1 km increments starting at 0.0 km and going to 19.9 km. Travel times needed in the program are computed from this table. Derivatives required are also determined by taking finite differences from the table. For estimated foci greater than 19.9 km from the station and/or deeper than 3.5 km, a straight line model is used.

The travel time curves are the P-wave travel times. The S-P, S and P phases are identified in the program as phases numbered 14, 15 and 16 respectively. The S and S-P

phases are computed by assuming

$$V_s = V_p / \sqrt{3}.$$

It should be noted that the travel time curves assume a flat surface of the earth. Elevation corrections are approximated in the Atime subroutine. For stations with elevations above 0.13 km, the correction term, ELEVC, assumes a constant velocity of 4.55 km/sec for the material above 0.13 km. For stations below 0.13 km, the velocity used is the average of 4.55 km/sec and the velocity at the station elevation. The correction term will have a maximum magnitude of approximately 0.01 sec.

#### Sample Output

The procedure for running the Locate program is as follows. The computer will print part of what follows. Comments are in parentheses.

RECOVER/SYSTEM: BATCH

/GET,DOALL/UN=GP301AF (GP301AF IS THE ACCOUNT THAT THE  
PROGRAM IS STORED UNDER.)

/GET,TAPE7/UN=GP301AF (TAPE7 IS THE FILE CONTAINING THE  
CLARK HILL TRAVEL TIME DATA. OTHER MODELS CAN BE  
INPUT HERE.)

/FTN,L=0,I=DOALL (L=0 PREVENTS THE PROGRAM FROM BEING  
PRINTED OUT.)



/LGO

FORMATS ARE FIELD FREE

IF NN=0 RETURN, =1 CONTINUE, =2 ADD STATION DATA

=3 ADD PHASE DATA, =4 LIST STATION DATA

=5 LIST PHASE DATA, =6 DEPTH SEQUENCE

=7 LIST PREVIOUS DATA, =8 RESTORE PREVIOUS DATA

=9 INTERCHANGE ROW DATA

READ NN

? (CHOOSE OPTION)

READ HR,MIN,SEC,ELAT,ELONG,DAY,MONTH,YEAR

? (ESTIMATED EPICENTER)

READ LABEL

?

READ EZ,WZ,WT,WX,WY,CDIST,NITER,SECERR,SMINER

? (EZ IS THE ESTIMATED DEPTH. THE W TERMS ARE THE WEIGHTS

ASSIGNED TO DEPTH, TIME AND HORIZONTAL COMPONENTS.

CDIST IS THE CONVERGENCE DISTANCE. NITER IS THE

NUMBER OF ITERATIONS ALLOWED. SECERR AND SMINER ARE

TIME ERROR CONTROLS.)

READ N,IPH,ID,SEC,SI

LAST N=NEGATIVE(NUMBER OF ENTRIES +1)

? (N IS A CONTROL NUMBER USED TO ORDER THE DATA. IPH IS THE

PHASE IDENTITY. ID IS THE STATION NUMBER. SEC IS THE

ARRIVAL TIME OF THE PHASE. HOUR AND MINUTES ARE TAKEN

FROM THE ESTIMATED EPICENTER INFORMATION. SI IS THE

TIME ACCURACY OF THE PHASE.)

```

SUBROUTINE ATIME(IIPH,TO,IO,ELAT,ELONG,EZ,C,RZ,IXX,XYZ)
  EZ POSITIVE DOWN  ELEV IS POSITIVE UP
  DIMENSION A(30),B(30),C(5),D(30),SLAT(200),SLONG(200),
  CELEV(200),IXX(2),XYZ(4),T(36,200),CC(30)
  STATION LATITUDE, LONGITUDE AND ELEVATIONS ARE STORED AS DATA
  STATEMENTS IN THIS SECTION. ADDITIONAL TEMPORARY STATIONS MAY
  BE ADDED BY USING THE NN=2 OPTION IN THE MAIN PROGRAM.
  VARIABLE NAMES USED ARE SLAT=STATION LATITUDE
  SLONG=STATION LONGITUDE, ELEV=STATION ELEVATION, A=PHASE
  VELOCITY, B=PHASE DELAY TIME (SEC), D=REFRACTOR DEPTH (KM),
  CC=DERIVATIVE OF TRAVEL TIME WITH RESPECT TO TIME
  FOR S-P PHASES CC=0.
  C(1)=THEORETICAL TRAVEL TIME, C(2)=DC(1)/DT, C(3)=DC(1)/DX,
  C(4)=DC(1)/DY, C(5)=DC(1)/DZ
  DATA(A(I),I=1,16)/3.550,5.800,6.2,3.7,6.5,4.5,8.3,2.6,4.55,
  C6.07,3.52,5.8,8.954,8.30,3.53,6.14/
  DATA(B(I),I=1,16)/0.0,0.0,0.0,2.7,0.8,12.0,8.2,0.0,0.0,0.0,
  C0.135,0.071,0.063,0.022,0.055,0.033/
  DATA(D(I),I=1,16)/0.0,0.0,0.0,25.0,25.0,40.0,40.0,0.0,0.0,
  C0.0,0.25,0.25,0.26,0.0,0.0,0.0,0.0/
  DATA(CC(I),I=1,16)/1.0,1.0,0.0,1.0,1.0,1.0,1.0,1.0,1.0,0.0
  C,1.0,1.0,0.0,0.0,1.0,1.0/
  THIS SECTION DETERMINES WHICH OPTION IS USED.
  IF IXX(1)=1, A TEMPORARY STATION IS ADDED.
  IF IXX(1)=2, A TEMPORARY PHASE IS ADDED.
  IF IXX(1)=3, A STATION LOCATION IS PASSED BACK TO THE MAIN
  PROGRAM.
  IF IXX(1)=4, A PHASE IS PASSED BACK TO THE MAIN PROGRAM.
  IF IXX(1)=5, THE TRAVEL TIME CURVE IS READ FROM TAPE 7.
  IF(IXX(1).EQ.1)GO TO 10
  IF(IXX(1).EQ.2)GO TO 20
  IF(IXX(1).EQ.3)GO TO 50
  IF(IXX(1).EQ.4)GO TO 60
  IF(IXX(1).EQ.5)GO TO 70
  SUBROUTINE CXY RETURNS THE EAST-WEST DISTANCE(X) AND THE
  NORTH-SOUTH DISTANCE (Y) FROM THE ESTIMATED EPICENTER TO THE
  STATION. X AND Y ARE IN KILOMETERS.
  CALL CXY(SLAT(IO),SLONG(IO),ELAT,ELONG,X,Y)
  R=SQRT(X*X+Y*Y)
  RZ=R
  IPH=IIPH
  XYZ(1)=1.0
  IF(IPH.GE.14.AND.IPH.LE.16)GO TO 80
  IF(IPH.GE.4)GO TO 29
  THIS SECTION ASSUMES THE RAYPATHS ARE STRAIGHT LINES.
15 RZ=SQRT(R*R+(EZ+ELEV(IO))*(EZ+ELEV(IO)))
  C(1)=CC(IPH)*TO+RZ/A(IPH)+B(IPH)
  C(2)=CC(IPH)
  C(3)=X/(A(IPH)*RZ)
  C(4)=Y/(A(IPH)*RZ)
  C(5)=(ELEV(IO)+EZ)/(A(IPH)*RZ)

```

```

RETURN
29 CONTINUE
  IF(D(IPH).LT.0.001)GO TO 15
    THIS SECTION IS FOR REFRACTED PHASES.
25 C(1)=CC(IPH)*TO+R/A(IPH)+B(IPH)*(2*D(IPH)+ELEV(ID)-EZ)/
  C(2*D(IPH))
  C(2)=CC(IPH)
  C(3)=X/(A(IPH)*R)
  C(4)=Y/(A(IPH)*R)
  C(5)=-B(IPH)/(2*D(IPH))
  RETURN
10 IX=IXX(2)
  SLAT(IX)=XYZ(1)
  SLONG(IX)=XYZ(2)
  ELEV(IX)=XYZ(3)
  RETURN
20 IX=IXX(2)
  A(IX)=XYZ(1)
  B(IX)=XYZ(2)
  CC(IX)=XYZ(4)
  D(IX)=XYZ(3)
  RETURN
50 IX=IXX(2)
  XYZ(1)=SLAT(IX)
  XYZ(2)=SLONG(IX)
  XYZ(3)=ELEV(IX)
  RETURN
60 IX=IXX(2)
  XYZ(1)=A(IX)
  XYZ(2)=B(IX)
  XYZ(3)=D(IX)
  XYZ(4)=CC(IX)
  RETURN
70 CONTINUE
  DO 73 I=1,36
  READ(7,71)DDD
73 READ(7,72)(T(I,J),J=1,200)
71 FORMAT(9X,F3.1)
72 FORMAT(10(1X,F8.5))
  RETURN

```

THIS SECTION USES THE CLARK HILL VELOCITY MODEL. THE DATA READ IN THE PRECEEDING SECTION IS USED HERE. FOCAL DEPTHS GREATER THAN 3.5 KM AND EPICENTER-STATION DISTANCES GREATER THAN 19.9 KM ARE SENT BACK TO THE FIRST SECTION.

```

80 IF(EZ.LT.-0.13)EZ=-0.13
  I=RI=10.*(EZ+0.13)+1.
  IF(I.GE.35)GO TO 15
  IF(R.GE.19.9)GO TO 15
  J=10.*R+1.
  D1=(T(I,J+1)-T(I,J))*(10.*R+1.-J)
  D2=(T(I+1,J+1)-T(I+1,J))*(10.*R+1.-J)

```

```

CON=1.00000
IF (IPH.EQ.14) CON=0.73205
IF (IPH.EQ.15) CON=1.73205
TR=(T(I+1,J)+D2-T(I,J)-D1)*(RI-I)
ELEV=(ELEV(ID)-0.13)/(4.8208-2.0833*ELEV(ID))
IF (ELEV(ID).GE.0.13) ELEV=(ELEV(ID)-0.13)*0.2198
TR=CON*(T(I,J)+D1+ELEV*TR)
C(1)=TR+IO*CC(IPH)
C(2)=CC(IPH)
D1=(T(I,J+1)-T(I,J))/0.1000
D2=(T(I+1,J+1)-T(I+1,J))/0.1000
DTDR=CON*(D1+(D2-D1)*(RI-I))
C(3)=X*DTDR/(R+0.00001)
C(4)=Y*DTDR/(R+0.00001)
D1=(T(I+1,J)-T(I,J))/0.100
D2=(T(I+1,J+1)-T(I,J+1))/0.100
C(5)=CON*(D1+(D2-D1)*(10.*R+1.-J))
RETURN
END

```

## APPENDIX D.

### Comparison of Earthquake Locations

This section compares earthquake locations obtained from the new model with the locations obtained from Denman's model. The table entries are arranged by the results of Denman's model and the results of the new model for the same event. The symbol DS on the depth indicates depth sequence. A time of 0.00 seconds indicates that the origin time was not computed.

Table 4. Comparison of Old and New Models.

Date	Time	Latitude	Longitude	Depth
9/18/74	3:12:52.86	33.9463	82.4968	1.85
	3:12:52.88	33.9464	82.4963	1.68
1/25/75	4:04:34.24	33.9488	82.5011	0.84
	4:04:34.26	33.9483	82.5021	0.50DS
1/25/75	4:24:51.93	33.9654	82.4919	0.79
	4:24:51.77	33.9536	82.4911	0.51
1/25/75	4:26:15.64	33.9671	82.4978	0.90
	4:26:15.67	33.9665	82.4985	0.85
2/23/75	4:04:34.14	33.9507	82.4954	1.62
	4:04:34.26	33.9487	82.5019	0.65
2/24/75	1:49:25.48	33.9554	82.4823	0.50DS
	1:49:25.50	33.9545	82.4849	0.00DS
2/24/75	4:09:19.02	33.9676	82.4891	0.00DS
	4:09:19.04	33.9653	82.4914	0.00DS
2/24/75	17:35:55.79	33.9637	82.4885	0.10DS
	17:35:55.82	33.9624	82.4911	0.10DS
2/24/75	17:38:21.54	33.9651	82.4847	0.00DS
	17:38:21.57	33.9633	82.4876	0.00DS
2/24/75	18:11:33.32	33.9377	82.4991	0.40DS
	18:11:33.35	33.9370	82.5014	0.00DS
2/24/75	18:30:19.11	33.9683	82.4915	0.25DS
	18:30:19.14	33.9665	82.4933	0.25DS
2/24/75	18:31:02.34	33.9677	82.4898	0.00DS
	18:31:02.37	33.9661	82.4927	0.00DS

Table 4. Continued

2/24/75	20:25:52.67	33.9674	82.4884	0.000S
	20:25:52.70	33.9657	82.4913	0.000S
2/24/75	23:35:01.77	33.9692	82.4958	0.250S
	23:35:01.79	33.9676	82.4977	0.250S
2/25/75	0:12:08.60	33.9763	82.4998	0.250S
	0:12:08.63	33.9744	82.5006	0.500S
2/25/75	0:45:24.38	33.9697	82.4989	0.250S
	0:45:24.40	33.9678	82.4999	0.500S
4/23/75	23:55:58.13	33.9507	82.4853	0.52
	23:55:58.15	33.9508	82.4869	0.45
4/24/75	2:08:15.26	33.9578	82.4963	0.92
	2:08:15.26	33.9575	82.4961	0.79
4/24/75	4:43:55.99	33.9593	82.4980	0.88
	4:43:55.00	33.9594	82.4971	0.68
4/24/75	5:18: 0.00	33.9665	82.5080	0.35
	5:18: 0.00	33.9649	82.5066	0.44
4/24/75	5:50:17.48	33.9588	82.4933	0.74
	5:50:17.49	33.9583	82.4935	0.55
4/24/75	5:52: 0.00	33.9592	82.4940	0.80
	5:52: 0.00	33.9587	82.4940	0.65
4/24/75	5:52:22.35	33.9580	82.4915	0.59
	5:52:22.36	33.9575	82.4922	0.30
4/24/75	5:53:36.11	33.9579	82.4908	0.45
	5:53:36.12	33.9572	82.4920	0.21

Table 4. Continued

4/24/75	6:27:59.35	33.9591	82.4919	0.71
	6:27:59.36	33.9585	82.4923	0.53
4/24/75	6:28:54.17	33.9579	82.4961	0.91
	6:28:54.18	33.9575	82.4961	0.78
4/24/75	15:33: 0.37	33.9574	82.4832	0.050S
	15:33: 0.38	33.9566	82.4905	0.200S
4/24/75	17:31:52.60	33.9595	82.4952	0.85
	17:31:52.61	33.9591	82.4951	0.70
4/24/75	18:50:27.53	33.9594	82.4937	0.76
	18:50:27.54	33.9589	82.4938	0.59
4/25/75	0:55:24.31	33.9558	82.4946	0.72
	0:55:24.32	33.9556	82.4949	0.51
4/25/75	4:14: 0.00	33.9545	82.5010	0.98
	4:14: 0.00	33.9544	82.5006	0.87
4/25/75	4:59:20.15	33.9583	82.4943	0.93
	4:59:20.16	33.9580	82.4942	0.80
4/25/75	5:01:07.74	33.9493	82.5032	0.75
	5:01:07.75	33.9497	82.5025	0.61
4/25/75	5:12: 0.00	33.9596	82.4899	0.42
	5:12: 0.00	33.9585	82.4913	0.200S
4/25/75	5:46:56.90	33.9564	82.4928	0.54
	5:46:56.91	33.9560	82.4937	0.34
4/25/75	17:50:49.79	33.9637	82.5059	0.96
	17:50:49.80	33.9631	82.5049	0.91



Table 4. Continued

4/25/75	18:10:01.23	33.9592	82.4999	1.21
	18:10:01.24	33.9589	82.4995	1.13
4/25/75	18:12:14.95	33.9572	82.5051	0.68
	18:12:14.96	33.9567	82.5041	0.54
4/25/75	18:20:43.59	33.9591	82.4940	0.82
	18:20:43.60	33.9586	82.4941	0.65
4/26/75	0:11:00.00	33.9417	82.4879	0.58
	0:11:00.00	33.9427	82.4889	0.58
4/26/75	0:25:34.21	33.9584	82.4958	1.00
	0:25:34.22	33.9580	82.4957	0.88
4/26/75	0:36:55.95	33.9586	82.4922	-0.050S
	0:36:55.97	33.9572	82.4944	0.200S
4/26/75	5:34:21.11	33.9604	82.4967	0.94
	5:34:22.12	33.9599	82.4965	0.81
4/26/75	6:54:57.91	33.9597	82.4967	0.90
	6:54:57.91	33.9593	82.4965	0.77
4/26/75	6:56:28.52	33.9571	82.4901	0.44
	6:56:28.53	33.9566	82.4914	0.17
4/26/75	7:24:31.38	33.9583	82.4952	0.89
	7:24:31.39	33.9580	82.4952	0.74
4/26/75	7:25:12.00	33.9620	82.4913	0.40
	7:25:12.01	33.9608	82.4923	0.200S
4/26/75	7:36:39.77	33.9596	82.4943	0.67
	7:36:39.78	33.9591	82.4946	0.50

Table 4. Continued

4/26/75	8:17:13.27	33.9601	82.4892	0.050S
	8:17:13.28	33.9587	82.4913	0.200S
4/26/75	8:25:10.58	33.9590	82.4908	-0.01
	8:25:10.59	33.9576	82.4931	0.200S
4/26/75	8:40:30.36	33.9578	82.4932	0.75
	8:40:30.37	33.9574	82.4934	0.56
4/26/75	17:36:06.13	33.9510	82.4974	0.27
	17:36:06.12	33.9510	82.4978	0.200S
4/26/75	18:12:31.87	33.9513	82.4966	0.12
	18:12:31.86	33.9511	82.4973	0.200S
5/21/75	6:47: 0.00	33.9491	82.4957	1.08
	6:47: 0.00	33.9494	82.4957	0.99
5/21/75	8:06: 0.00	33.9578	82.4980	1.33
	8:06: 0.00	33.9576	82.4978	1.26
5/21/75	8:06: 0.00	33.9562	82.4916	1.32
	8:06: 0.00	33.9561	82.4916	1.24
5/21/75	9:12: 0.00	33.9515	82.5049	0.85
	9:12: 0.00	33.9516	82.5041	0.73
5/21/75	22:56: 0.00	33.9537	82.5093	1.70
	22:56: 0.00	33.9536	82.5086	1.66
5/22/75	1:34: 0.00	33.9601	82.5132	1.13
	1:34: 0.00	33.9597	82.5121	1.12
5/22/75	8:09: 0.00	33.9629	82.5093	1.07
	8:09: 0.00	33.9623	82.5083	1.05

Table 4. Continued

5/22/75	10:53: 0.00	33.9560	82.5017	0.75
	10:53: 0.00	33.9557	82.5012	0.59
5/22/75	20:26: 0.00	33.9626	82.4984	0.56
	20:26: 0.00	33.9613	82.4981	0.42
5/23/75	7:19: 0.00	33.9566	82.4992	1.03
	7:19: 0.00	33.9564	82.4989	0.92
5/23/75	7:19: 0.00	33.9545	82.4993	0.98
	7:19: 0.00	33.9544	82.4990	0.87
5/23/75	8:01: 0.00	33.9604	82.5068	2.13
	8:01: 0.00	33.9602	82.5064	2.11
3/26/77	2:04:3.19	33.9598	82.4967	1.16
	2:04:3.23	33.9610	82.4964	0.94
3/26/77	3:49:57.61	33.9609	82.5009	0.98
	3:49:57.64	33.9628	82.5014	0.85
3/26/77	5:28:25.81	33.9596	82.5063	0.83
	5:28:25.85	33.9634	82.5075	0.72
3/26/77	5:48:44.81	33.9684	82.5037	0.19
	5:48:44.81	33.9674	82.5073	0.100S
3/26/77	6:50:55.95	33.9599	82.5076	1.04
	6:50:55.99	33.9646	82.5089	0.90
3/26/77	7:43:20.04	33.9595	82.5054	0.86
	7:43:20.08	33.9631	82.5065	0.76
3/26/77	18:12:13.08	33.9612	82.5078	0.83
	18:12:13.11	33.9654	93.5082	0.59

Table 4. Continued

3/26/77	19:04:57.66	33.9584	82.4987	1.96
	19:04:57.71	33.9631	82.4982	1.83
3/26/77	19:17:20.72	33.9595	82.5045	0.88
	19:17:20.76	33.9627	82.5054	0.80
3/26/77	19:43:16.40	33.9583	82.5064	0.21
	19:43:16.42	33.9624	82.5078	0.10DS
3/26/77	19:48:3.62	33.9587	82.5023	0.41
	19:48:3.64	33.9613	82.5040	0.41
3/26/77	20:42:41.42	33.9635	82.5042	0.59
	20:42:41.44	33.9653	82.5057	0.38
4/13/77	1:05:29.81	33.9645	82.5040	0.10
	1:05:29.79	33.9633	82.5039	0.05DS
4/14/77	12:54:33.10	33.9530	82.5124	1.62
	12:54:33.11	33.9532	82.5122	1.59
4/14/77	16:22:42.44	33.9616	82.4982	0.86
	16:22:42.50	33.9609	82.4972	0.78
4/14/77	16:45:40.00	33.9674	82.5070	1.02
	16:45:40.01	33.9669	82.5068	0.95

# BIBLIOGRAPHY

- Aki, K. and W. H. K. Lee, Determination of Three-Dimensional Velocity Anomalies Under a Seismic Array Using First P Arrival Times From Local Earthquakes, J. Geophys. Res., 81(23), 4381-4399, 1976.
- Birch, F., The Velocity of Compressional Waves in Rocks to 10 Kilobars, Part 1, J. Geophys. Res., 65(4), 1083-1102, 1960.
- Bridges, S. R., Evaluation of Stress Drop of the August 2, 1974 Georgia-South Carolina Earthquake and Aftershock Sequences, Master's thesis, Georgia Institute of Technology, 1975.
- Denman, H. E., Jr., Implications of Seismic Activity at the Clark Hill Reservoir, Master's thesis, Georgia Institute of Technology, 1974.
- Dorman, Leroy M., Seismic Crustal Anisotropy in Northern Georgia, Bull. Seismol. Soc. Amer., 62(1), 39-45, 1972.
- Garland, G. D., Introduction to Geophysics, 24-28 and 54-56 W. B. Saunders Co., 1971.
- Guinn, S. A., Master's Thesis, in progress, Georgia Institute of Technology, 1977.
- Guinn, S. A., Travel Time Curve for the Georgia Piedmont. Unpublished report, 1976.
- Marion, G. E., A Spectral Analysis of Microearthquakes That Occur in the Southeastern United States, Master's thesis, Georgia Institute of Technology, 1977.
- Leary, P., P. Malin, R. A. Phinney and R. VonColln, Seismic Travel Time Experiment With Air Gun Source, Clark Hill Reservoir, South Carolina, March 1975, Field Report, Princeton University, 1975.
- Long, L. T., Earthquake Sequences and b Values in Southeast United States, Bull. Seismol. Soc. Amer., 64(1), 267-273, 1974.
- Stewart, Roger and L. Pešelnick, Velocity of Compressional Waves in Dry Franciscan Rocks to 8 kbar and 300 C, J. Geophys. Res., 82(14), 2027-2039, 1977.